EFFECT OF THERMAL RADIATION ON MIXED CONVECTIVE HEAT AND MASS TRANSFER FLOW OF A ROTATING NANO FLUID IN A VERTICAL CHANNEL WITH STRETCHING WALL IN THE PRESENCE OF HEAT SOURCES

[1] **Dr. M. Gayathri**
[1] Assistant Professor
[1] Department of Mathematics
[1] Government First Grade College, Varthur, Bangalore-560087, Karnataka, India.

*Abstract :*The present investigation deals with the boundary layer flow, heat and mass transfer of rotating nanofluid in a vertical channel bounded by a stretching and stationary walls under the influence of a uniform magnetic field. Similarity transformations are used to convert the governing partial differential equations into a system of non-linear ordinary differential equations and are solved numerically by using shooting method. The effects of magnetic field, radiation parameter, chemical reaction parameter, Eckert number, rotation parameter, heat source parameters, Brownian motion parameter, thermophoresis parameter, Prandtl number on the velocity, temperature and concentration fields are discussed numerically through graphs and tables.

Index terms: Radiation, Heat and Mass transfer, Rotating fluid, stretching wall, Non-uniform heat sources.

I. INTRODUCTION

Study of convective heat transfer in nanofluids has become a topic of contemporaneous interest due to its applications in several industries such as power plant operations, manufacturing and transportation, electronics cooling, heat exchangers. The word “nanofluid” coined by Choi [8] refers to a liquid suspension containing ultra - fine particles (diameter less than 50 nm). The traditional fluids used for heat transfer applications such as water, mineral oils, ethylene glycol, engine oil have limited heat transfer capabilities. The nanofluids which are the engineered colloidal suspension of nano meter sized particle of metals and metallic oxides such as Aluminium, Copper, Gold, Iron and Titanium or their oxides in base fluids. The base fluids are usually water, oil, ethylene glycol, bio fluids and toluene. Experimental investigations revealed that base fluids with suspension of the nano particles have substantially higher thermal conductivities than those of the base fluids.

Eastman et al. [11] and Minsta [29] showed that even with small volumetric fraction of nano particles (less than 5%), the thermal conductivity of the base liquid can be enhanced by 10 - 50%. It was reported that a small amount (less than 1% volume fraction) of copper nano particles or carbon nano tubes dispersed in ethylene glycol or oil can increase their inherently poor thermal conductivity by 40% and 50% respectively (Eastman et al., [12]; Choi et al., [7]). The unique properties of these nanofluids made them potential to use in many applications in heat transfer. A recent application of the nanofluid as suggested by Kleinstreuer et al.,[23] is in delivery of nano-drug. Eastman et al., [11] attributed the enhancement of thermal conductivity to the increase in surface area due to the suspension of nanoparticles. Keblinski et al., [20] discussed on the possible mechanisms for the improved thermal conductivity. According to them the contribution of Brownian motion is much less than other factors such as size effect, clustering of nanoparticles and surface adsorption.

Boungiorno [5] evaluated the different theories explaining the enhanced heat transfer characteristics of nanofluids. He developed an analytical model for convective transport in nanofluids which takes into account the Brownian diffusion and thermophoresis. Using this model, Kuznetsov and Nield [25] investigated the natural convective flow of a nanofluid over a vertical plate. Bachok et al. [3] numerically studied steady boundary layer flow of a nanofluid over a moving semi-infinite plate in a uniform free stream. Effect of magnetic fuel on free convection flow of a nanofluid past a vertical semi-infinite flat plate has been discussed by Hamad et al. [16]. Gorla and Chamkha [14] investigated natural convection flow past a horizontal plate in a porous medium filled with a nanofluid.

The fluid flow due to a stretching surface has important applications such as production of glass and paper sheets, metal spinning, hot rolling, drawing of plastic films, and extrusion of metals and polymers. Khan and Pop [22] studied the boundary layer flow of a nanofluid past a stretching sheet. The heat and mass transfer analysis for boundary layer stagnation – point flow over a stretching sheet in a porous medium saturated by a nanofluid with internal heat generation/absorption and suction/blowing is investigated by Hamad and Ferdows[17]. Nadeem and Lee [33] made an analytical investigation of the problem of steady boundary layer flow of a nanofluid over an exponential stretching surface including the effects of Brownian motion and thermophoresis. Makinde and Aziz [28] studied the boundary layer flow of a nanofluid past a stretching sheet with a convective boundary condition.

Rana and Bhargava [35] analyzed numerically the flow and heat transfer of a nanofluid over a nonlinearly stretching sheet. Sulochana et al[39] have analysed the effect of heat sources on non-Darcy convective heat and mass transfer flow of Cuo-water and Al_2O_3-water nanofluids in vertical channel. The study of magneto hydrodynamics has significant applications in engineering. MHD generators, devices in petroleum industry, material processing, nuclear reactors etc are some applications. The use of magnetic fields plays an important role in the process of purification of molten metals from non metallic inclusions. The MHD fluid flow in a rotating channel is an interesting area in the study of fluid mechanics because of its relevance to various engineering applications.

It is challenging approach to atmospheric science that exerts its influence of rotation to help in understanding the behaviour of oceanic circulation and formation of galaxies. The effect of Coriolis force in the atmosphere is exposed to oceanic circulation and the formation of galaxies in taking into account the flow of electron is continuously liberated from the sun what is called "solar wind". The MHD flow in the rotating environment leads to a start up process implying thereby a viscous layer at the boundary is suddenly set into motion and the rate of rotation becomes important in the application of various branches of geophysics, astrophysics and fluid engineering. Zanchini [40] has discussed the effect of viscous dissipation on mixed convection in a vertical channel with boundary conditions of the third kind.

Mahendra Mohan [31] has discussed the free and forced convections in rotating Hydro magnetic viscous fluid between two finitely conduction parallel plates maintained at constant temperature gradients. In view of many scientific and engineering applications of fluids flow through porous media, Mahendra Mohan and Srivastava [32] have studied the combined free and forced convection flow of an incompressible viscous fluid in a parallel plates channel bounded below by a permeable bed and rotating with a constant angular velocity about an axis perpendicular to the length of the plates. Rao et.al. [34] made an investigation of the combined free and forced convective effects on an unsteady Hydro magnetic viscous incompressible flow in a rotating porous channel. This analysis has been extended to porous boundaries by Sarojamma and Krishna [36].

An initial value investigation of the hydro magnetic and convective flow of a viscous electrically conducting fluid through a porous medium in a rotating channel has been made by Krishna et.al. [24]. In all these papers the viscous dissipative effect has not been considered. But the viscous dissipation has its importance when the natural convection flow fixed is of extreme size or the temperature is low or in higher gravity field. The problem of steady laminar micro polar fluid flow through porous walls of different permeability had been discussed by Agarwal and Dhanpal [1]. Steady and unsteady hydro magnetic flow of viscous incompressible electrically conducting fluid under the influence of constant and periodic pressure gradient in the presence of include magnetic field have been study by several authors [2, 6, 10, 15, 19, 22, 30, 37] the effect of slowly rotating systems with low frequency of oscillation when the conductivity of the fluid is low and the applied magnetic field is weak.

El-Mistikawy et.al. [13] were discussed the rotating disk flow in the presence of strong magnetic field and weak magnetic field. Hazim Ali Attia [18] was developed the MHD flow of incompressible, viscous and electrically conducting fluid above an infinite rotating porous disk was extended to flow starting impulsively from rest. The fluid was subjected to an external uniform magnetic field perpendicular to the plane of the disk. The effects of uniform suction or injection through the disk on the unsteady MHD flow were also considered. Circar and Mukherjee [9] have analyzed the effect of mass transfer and rotation on flow past a porous plate in a porous medium with variable suction in a slip flow regime.

Balasubramanyam [4] and Reddy [27] have investigated convective heat and mass transfer flow in horizontal rotating fluid under different conditions. Singh and Mathew [37] have studied on oscillatory free convective MHD flow in a rotating vertical porous channel with heat sources. Recently, Pudi Sreenivasa Rao[38] has discussed the effect of chemical reaction and dissipation on MHD convective heat and mass transfer flow in a vertical channel bounded by stretching and stationary walls in the presence of heat sources. Madhavi et al[26] have investigated heat and mass transfer flow of a rotating fluid in a vertical channel with stretching and stationary walls.

The present investigation deals with the boundary layer flow, heat and mass transfer of rotating nanofluid in a vertical channel bounded by a stretching and stationary walls under the influence of a uniform magnetic field. Similarity transformations are used to convert the governing partial differential equations into a system of non-linear ordinary differential equations and are solved numerically by using shooting method. The effects of magnetic field, radiation parameter, chemical reaction parameter, Eckert number, rotation parameter, heat source parameters, Brownian motion parameter, thermophoresis parameter, Prandtl number on the velocity, temperature and concentration fields are discussed numerically through graphs and tables.

2. FORMULATION OF THE PROBLEM:

We consider the steady two dimensional hydromagnetic laminar convective heat and mass transfer flow of a viscous electrically conducting fluid in a vertical channel bounded by a stretching sheet on the left a stationary plate on the right. We choose a rectangular coordinate system O(x,y.z) with the walls at $y=\pm L$ .a uniform magnetic field of strength Ho is applied normal to the walls. Assuming magnetic Reynolds number (Rm) to be small we neglect the induced magnetic field in comparison to the applied magnetic field. It is used to compare the transport of magnetic lines of the force in a conducting fluid with the leakage of such lines from the fluid. For a small magnetic Reynolds number, the magnetic field will tend to relax towards a purely diffusive state. It is also assumed that there is no applied polarization and hence no electric field. The body couple is assumed to be absent.

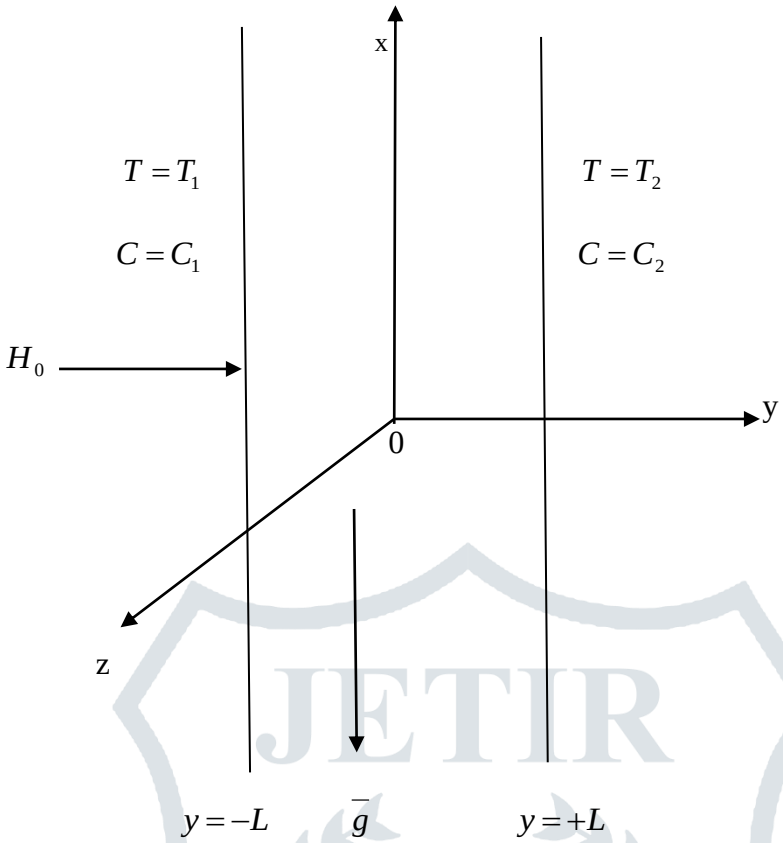

Fig.1 : Configuration of the problem

We, therefore, may express the velocity, temperature, concentration in the following form

$$\bar{q} = (u(x,y), v(x,y), w(x,y)), T = T(x,y), C = C(x,y) \tag{1}$$

Taking the viscous dissipation and joule heating effects into consideration, the governing equations of the flow, heat and mass transfer for the problem are

$$\frac{\partial u}{\partial x} + \frac{\partial v}{\partial y} = 0 \tag{2}$$

$$u\frac{\partial u}{\partial x} + v\frac{\partial u}{\partial y} = -\frac{1}{\rho_f}\frac{\partial p}{\partial x} + \nu\left(\frac{\partial^2 u}{\partial x^2} + \frac{\partial^2 u}{\partial y^2}\right) + \left(\frac{2\Omega}{\rho_f}\right)w - (\sigma\mu_e^2 H_o^2/\rho_f)u + \frac{1}{\rho_f}[(1-C_o)\rho_f \beta g(T-T_2)] - \frac{(\rho_p - \rho_f)g(C-C_o)}{\rho_f} \tag{3}$$

$$u\frac{\partial v}{\partial x} + v\frac{\partial v}{\partial y} = -\frac{1}{\rho_f}\frac{\partial p}{\partial y} + \nu\left(\frac{\partial^2 v}{\partial x^2} + \frac{\partial^2 v}{\partial y^2}\right) \tag{4}$$

$$u\frac{\partial w}{\partial x} + v\frac{\partial w}{\partial y} = \nu\left(\frac{\partial^2 w}{\partial x^2} + \frac{\partial^2 w}{\partial y^2}\right) - (\sigma\mu_e^2 H_o^2/\rho_f)w - \left(\frac{2\Omega}{\rho_f}\right)u \tag{5}$$

$$u\frac{\partial T}{\partial x} + v\frac{\partial T}{\partial y} = \frac{k_f}{\rho_f C_p}\left(\frac{\partial^2 T}{\partial x^2} + \frac{\partial^2 T}{\partial y^2}\right) + \tau\left\{D_B\frac{\partial T}{\partial y}\frac{\partial C}{\partial y} + \frac{D_T}{T_\infty}\left(\frac{\partial T}{\partial y}\right)^2\right] + q''' - \frac{\partial (q_R)}{\partial y} + \frac{2\mu}{\rho_f C_p}\left(\left(\frac{\partial u}{\partial y}\right)^2\left(\frac{\partial w}{\partial y}\right)^2\right) + \left(\frac{\sigma\mu_e^2 H_o^2}{\rho_f C_p}\right)(u^2 + w^2) \tag{6}$$

$$u\frac{\partial C}{\partial x} + v\frac{\partial C}{\partial y} = D_B\left(\frac{\partial^2 C}{\partial x^2} + \frac{\partial^2 C}{\partial y^2}\right) - kc(C - C_0) + \frac{D_T k_T}{T_m}\left(\frac{\partial^2 T}{\partial x^2} + \frac{\partial^2 T}{\partial y^2}\right) \tag{7}$$

$$\rho - \rho_o = -\beta(T - T_o) - \beta^*(C - C_o) \tag{8}$$

Where(u,v.0) are the velocity components along x,y directions respectively, T,C are the dimensional temperature and nanoparticle concentration respectively, ρ is the density, p is the pressure,σ is the electrical conductivity, μ_e is the magnetic permeability of the medium, μ is the dynamic viscosity, k is the permeability of the porous medium, g is the gravity, D_B is the Brownian diffusion coefficient, D_T is the Thermophoretic diffusion coefficient, K_T is the thermal diffusion ratio, β is the coefficient of thermal expansion, β^* is the coefficient of volume expansion, Tm is the mean fluid temperature. $\tau = \frac{(\rho C_p)_p}{(\rho C_p)_f}$ is the ratio of nanoparticle heat capacity and base fluid heat capacity.

The coefficient q''' is the rate of internal heat generation (>0) or absorption(<0). The internal heat generation /absorption q''' is modelled as

$$q''' = \frac{k_f us}{x\nu}(A11(T_1 - T_2)u + B11(T - T_2)) \tag{9}$$

Where A11 and B11 are coefficients of space dependent and temperature dependent internal heat generation or absorption respectively. It is noted that the case A11>0 and B11>0, corresponds to internal heat generation and that A11<0 and B11<0, the case corresponds to internal heat absorption case.

The radiation heat term by using the Rosseland approximation is given by

$$q_r = -\frac{4\sigma^\bullet}{3\beta_R}\frac{\partial T'^4}{\partial y},\quad T'^4 \cong 4TT_o^3 - 3T_0^4,\quad \frac{\partial q_R}{\partial z} = -\frac{16\sigma^\bullet T_0^3}{3\beta_R}\frac{\partial^2 T}{\partial y^2} \tag{10}$$

where $\sigma^\bullet$ is the Stefan-Boltzman constant and β_R mean absorption coefficient.

The boundary conditions for the velocity, temperature and concentration are

$$\begin{aligned} &u(x,-L) = bx, u(x,+L) = 0, v(x,\pm L) = 0, \\ &T(x,-L) = T_1, T(x,+L) = T_2 \\ &C(x,-L) = C_1, C(x,+L) = C_2 \end{aligned} \tag{11}$$

where b>0 is the stretching rate of the channel wall T_1 , T_2 (with ($T_1 > T_2$)are the fixed temperature of the left and right walls respectively, C_1, C_2 (with $C_1 > C_2$) or the fixed concentrations of the channel walls respectively. We introduce the following Similarity variables as:

$$\begin{aligned} &\eta = \frac{y}{L}; u = bxf'(\eta); v = -bLf(\eta), w = bxg(\eta) \\ &\theta(\eta) = \frac{T - T_2}{T_1 - T_2}, \phi(\eta) = \frac{C - C_2}{C_1 - C_2} \end{aligned} \tag{12}$$

The above velocity field is compatible with continuity equation(2) and therefore ,represents the possible fluid motion.

Eliminating the pressure between the equations (3)and (4) and using(10) the momentum equation reduces to

$$f^{iv} + \mathrm{Re}\, x(f'''f' - ff'') - M^2 f'' + Gr(\theta' - N\phi') + Rg' = 0 \tag{13}$$

$$g'' + \mathrm{Re}\, x(fg' - f'g) - M^2 g - Rf' = 0 \tag{14}$$

whereas the equations (6) & (7) in view of equation(9),(10) &(12) are

$$\begin{aligned} &(1 + \frac{4Nr}{3})\theta'' + \Pr \mathrm{Re}\, x(f\theta') + A_1 f' + B_1\theta + \Pr Ec((f'')^2 + (g')^2) + \\ &\quad + M^2 Ec((f')^2 + g^2) + \Pr Nb(\theta'\phi') + \Pr Nt(\theta'^{2)} \end{aligned} \tag{14a}$$

$$\phi'' + Le\,\mathrm{Re}\, x(f\phi') - Le\gamma(\phi) + (\frac{Nt}{Nb})\theta'' = 0 \tag{14b}$$

Where $Gr = \frac{\beta g(T_1 - T_2)L}{bx}$ is the Grashof number, $N = \frac{(\rho_p - \rho_f)(C_1 - C_2)}{(1 - C_o)\rho_f \beta(T_1 - T_2)}$ is the buoyancy ratio parameter, $M^2 = \frac{\sigma\mu_e^2 H_o^2 L^2}{\nu x}$ magnetic parameter, $\Pr = \frac{\mu C_p}{k_f}$ is Prandtl number, $A_{11} = \frac{A_1 b^2 x}{\nu}$ is the space dependent heat source parameter, $B_{11} = \frac{B_1 b}{\nu}$ is the temperature dependent heat source parameter, $\mathrm{Re}\, x = \frac{bL^2}{\mu}$, is the local Reynolds

number, $Le = \frac{\nu}{D_B}$ is the Lewis number, $S_r = \frac{D_T K_T (T_1 - T_2)}{T_m (C_1 - C_2)}$ is the Soret parameter, $\gamma = \frac{kcL^2}{D_B}$ is the chemical reaction parameter, $Ec = \frac{b^2 x^2}{C_p \Delta T}$ is the Eckert number, $Nr = \frac{4\sigma^{\bullet} T_o^3}{\beta_r k_f}$ is the radiation parameter, $Nt = \frac{(\rho C_p)_p D_T (T_1 - T_2)}{(\rho C_p)_f T_o \nu}$ is the thermophoretic parameter, $Nb = \frac{(\rho C_p)_p D_B (C_1 - C_2)}{(\rho C_p)_f \nu}$ is the Brownian motion parameter.

Boundary conditions(11), in view of equation (12) in dimensional form reduces to

$$f(\pm 1) = 0,\ f'(-1) = 1,\ f'(+1) = 0,\ \text{g(-1)=0,g(+1)=0,}\ \theta(-1) = 1, \theta(+1) = 0\ ,\ \phi(-1) = 1, \phi(+1) = 0 \qquad (14c)$$

3. METHOD OF SOLUTION:

A usual approach is to write the nonlinear ODE in form of a first order initial value problem as follows:

$$f = f_1,\ f' = f_2\ f'' = f_3,\ f''' = f_4, g = f_5, g' = f_6$$
$$\theta = f_7, \theta' = f_8, \phi = f_9, \phi' = f_{10} \qquad (15)$$

$$f^{iv} = f_4' = -\mathrm{Re}\, x[f_4 f_1 - f_2 f_3] + M^2 f_3 + Gr(f_6 - N f_8) - Rg' \qquad (16)$$

$$g'' = f_6' = -\mathrm{Re}\, x[f_6 f_1 - f_2 f_5] + M^2 f_5 + R f_2 \qquad (17)$$

$$\theta'' = f_8' = -[\mathrm{Pr}\,\mathrm{Re}\, x(f_1 f_8) + A_{11} f_2 + B_{11} f_7 - \mathrm{Pr}\, Ec(f_3^2 + f_6^2) - M^2 Ec(f_2^2 + f_5^2) - \mathrm{Pr}\, Nb(f_8 f_{10}) - \mathrm{Pr}\, Nt(f_8^2)]/(1 + \frac{4Nr}{3}) \qquad (18)$$

$$\phi'' = f_8' = [-Le\,\mathrm{Re}\, x(f_1 f_{10}) + Le\gamma\ f_9 - (\frac{N_t}{N_b})(-[\mathrm{Pr}\,\mathrm{Re}\, x(f_1 f_8) + A_{11} f_2 + B_{11} f_7 - \mathrm{Pr}\, Ec(f_3^2 + f_6^2) - M^2 Ec(f_2^2 + f_5^2) - \mathrm{Pr}\, Nb(f_8 f_{10}) - \mathrm{Pr}\, Nt(f_8^2)]/(1 + \frac{4Nr}{3})) \qquad (19)$$

The corresponding boundary conditions are

$$f_1(\pm 1) = 0,\ f_2(-1) = 1,\ f_2(+1) = 0,\ f_5(-1) = 1,\ f_5(+1) = 0,\ f_6(-1) = 1,\ f_6(+1) = 0,\ f_7(-1) = 1,$$
$$f_7(+1) = 0,\ f_8(-1) = 0,\ f_8(+1) = 0 \qquad (20)$$

Here $f_3(-1), f_4(-1), f_6(-1), f_8(-1), f_{10}(-1)$ are the unknown initial condition, Therefore, a shooting methodology is incorporated to solve the above system, which may be a combination of the Runge-Kutta method (to solve first order ODE) and a five dimensional zero finding algorithm(to find the missing coordinates). It is note that the missing initial conditions are coupled so that the solution satisfies the boundary conditions f(+1)=0, f'(+1)=0, g(+1)=0, θ(+1)=0, $\phi(+1) = 0$ of the original boundary value problem.

4. DISCUSSION OF NUMERICAL RESULTS:

In this analysis we investigate the influence of non-uniform heat sources on convective heat and mass transfer flow of a viscous, dissipative rotating fluid in a vertical channel bounded by a stretching sheet and stationary plates. The non-linear governing equations have been solved by employing Fourth order Runge - Kutta –Shooting technique. The velocity, temperature and concentration have been analysed for different variations of G, M, N, A11, B11, Nr, R, Ec, Nb, Nt, γ and Pr.

Rotating channel-am=0-case

The effect of free convection parameter G on the velocity is depicted in Fig.2a & 2b when Nr = 0.1, Pr = 0.71, Nb = 0.3, Nt = 0.3, Nr=0.5, Le = 1, A11=0.1, B11=0.1, γ=0.5,Ec=0.01,R=0.5, M = 0.5. From this figure it is observed that the primary and secondary velocities increase monotonically to zero as the distance η increases from the boundary. An increase in G results in the enhancement of both the velocities due to the enhancement of convection currents and thus thickness of the boundary layer increases. An increase in the

value of G amounts to an increase in the temperature difference which leads to the enhancement convection currents and thus facilitates to increase the velocities consequently the thickness of the boundary layer increases. Fig. 3a & 3b illustrate the influence of magnetic field.

It is observed that the presence of magnetic field reduces the velocities throughout the boundary layer which is in the conformity with the fact that the Lorentz force or magnetic force acts as a retarding force. Higher the Lorentz force lesser is the velocity.Figs.4a & 4b show the variation of velocities with buoyancy ratio(N). The velocities increase for increasing values of buoyancy ratio (Fig. 4a) and hence an enhancement in the thickness of the boundary layer is noticed. It is found that when the molecular buoyancy force dominates over the thermal buoyancy force the velocities enhance in the flow region. From figs.5a & 5b we find that an increase in rotation parameter(R)increases both the primary and secondary velocities. Thus higher the angular velocity larger the thickness of the boundary layer which results to an enhancement in the velocity in the flow region. From Fig. 6a & 6b it is observed that the presence of radiation (Nr) increases the velocity. Further increase in the radiation parameter facilitates the enhancement of both the velocities and thus increases the thickness of the boundary layer.

From Fig. 7a & 7b it is observed that the influence of Nt is to increase the velocities as in the case of temperature. The effect of Brownian motion parameter (Nb) on velocity is depicted in Fig. 8a & 8b. Increase in Nb enhances the primary velocity and reduces the secondary velocity and hence the thickness of the hydrodynamic boundary layer enlarges. From Fig. 9a & 9b, it is observed that for increasing values of suction parameter fw the primary velocity experiences depreciation while it enhances with injection parameter (fw<0).The secondary velocity(g) increases with increasing values of suction/injection parameter(fw). Figs.10a & 10b represent the variation of velocities with space dependent heart source parameter(A11). It is found that with increase in A11>0,both the velocities enhance while for A11<0,the primary velocity increases while the secondary velocity reduces in the flow region. The effect of temperature dependent heat source parameter(B11) on velocities is shown in figs.11a & 11b.In the presence of heat generating source, heat is generated in the flow region which increases the both the velocities. In the case of heat absorbing source(B11<0),the primary and secondary velocities decrease due to the absorption of heat energy. The effect of dissipation on the velocities is depicted in figs.12a &12b.It can be seen from the profiles that higher the dissipative energy larger the magnitude of the velocities in the flow region.

Figs 13a & 13b represent the velocities with chemical reaction parameter(γ). The primary velocity increases and the secondary velocity reduces in the degenerating chemical reaction case while both the velocities enhances in the generating chemical reaction case. The effect of Lewis number(Le) on velocities is shown in figs.14a & 14b.It can be seen from the profiles that an increase in Le grows the thickness of the boundary layer which in turn enhances the both the velocities in the flow region. Fig. 15a &15b illustrates the effect of Prandtl number on velocities for a selected value of remaining parameters. It is found that both the velocities depreciate the velocities leading to a reduction in the hydrodynamic boundary layer.

Fig. 2c shows that an increase in free convection parameter (G) decreases with temperature. It is observed that (Fig.4c) the temperature decreases significantly for increasing values of the buoyancy ratio, which is in conformity with the fact that the buoyancy ratio facilitates the reduction of the heat transfer and hence the thickness of the thermal boundary layer reducers qualitatively. From Fig. 3c the thermal boundary layer thickness is observed to decrease with increasing values of the Lorentz force. The thermal boundary layer thickness decreases with increasing N.

Fig. 6c presents the effect of radiation parameter on temperature. Increasing values of Nr enhance the temperature leading to an increase in the thickness of the thermal boundary layer. The temperature steadily increases for an increase in Brownian motion parameter Nb(fig.8c).The effect of thermophoresis parameter Nt on θ is depicted in Fig. 7c. It is observed that the temperature increases more for increasing values of Nt in the flow region. From Fig. 9c it is observed that for increasing values of suction parameter the temperature decreases while3 it increases with injection parameter(fw<0). Fig. 10c shows the effect of the space dependent heat source parameter (A11)on the temperature .From the profiles we find that the temperature enhances with increasing A11>0 and reduces with deceasing values of A11<0.

Fig.11c shows the variation of θ with temperature dependent heat source parameter(B11).In the presence of heart generating heat source, heat is generated which in turn enhances the temperature in the

flow region, while the temperature reduces due to the absorption of heat energy. From fig.12c we notice an enhancement in the temperature in the flow region with higher dissipative energy.Fig.13c shows the variation of θ with chemical reaction parameter(γ).From the figure we find that the temperature reduces in the degenerating chemical reaction case while it enhances in the case of generating chemical case. The effect of Lewis number on temperature (Fig. 14c) is to increase the temperature in the flow region of the thermal boundary layer. From Fig. 15c it is observed that the increasing values of Prandtl number reduce the temperature significantly .

Concentration increases (Fig. 2d) with increasing values of the free convection parameter (G). From Fig. 4d it is observed that the volume fraction of the nano particles is decreased with increase in the buoyancy ratio in the flow region. It is observed that the increase in the magnetic parameter (Fig. 3d) increases the concentration of the nanoparticles considerably. From Fig. 6d it is observed that for increasing values of radiation parameter the volume fraction of the nano particles is reduced. From Fig. 7d it is noticed that increasing values of thermophoresis parameter (Nt) reduces moderately the nanoparticle concentration.The effect of the Brownian motion parameter(Nb) (Fig. 8d) is to reduce the concentration. From Fig. 9d it is observed that the nanoparticle concentration increases with increasing values of suction parameter(fw>0) and reduces with injection parameter(fw<0).

It is observed that (Fig. 10d &11d) nanofluid concentration reduces with increase in A11>0 & B11>0 and enhances with incre4ase in A11<0 & B11<0. Higher the dissipative energy smaller the concentration in the flow region(fig.12d).The concentration reduces in the degenerating chemical reaction and enhances in the generating case(fig.13d). From Fig.14d it is observed that the increasing values of Lewis number increase very significantly the concentration. An increase in Prandtl number(Pr) enhances the nanoparticle concentration (fig.15d).

The skin friction, Nusselt number and Sherwood number are tabulated in table (2). From this table it is observed that an increase in the free convection parameter (G)leads to an increase in the skin friction component(τx) and enhances τz at the walls. Nusselt number enhances and Sherwood number reduces with G. The buoyancy ratio decreases the values of skin friction component τx and enhances τz, Nusselt number and Sherwood number when the buoyancy forces are in the same direction and for the forces acting in opposite directions,τx,and Sh reduces ,while τz and Nu enhances on the wall .

The effect of magnetic field is to reduce the skin friction component τz and Nu ,increases τx and Sh. The radiation parameter enhances the values of skin friction component τz and Sh while τx and Nu reduces on the wall.. The effect of Brownian motion parameter on the skin friction and Sherwood number is to increase while it decreases the Nusselt number. This is due to the enhancement in velocity and temperature and reduction in the concentration. The thermophoresis parameter decreases the values of skin friction, Nusselt number and Sherwood number. The space/temperature dependent heat source parameters(A11,B11) reduces the skin friction τx, Nu and enhances τz and Nu on the wall in case of heat source/heat generating source, while reversed effect is noticed with that heat sink/absorbing source. The effect of Lewis number is to increase the skin friction components, Nusselt number while it decreases the Sherwood number on the wall. Effect of rotation parameter (R)is to increase the skin friction components and reduces the Nusselt and Sherwood numbers on the wall.

Higher the dissipation smaller the skin friction component τx and Nu and enhances τz and Sh on the wall. τx and Sh reduces with Nt and enhances with Nb. An increase in Nb and Nt enhances τz and Nu on the wall. An increase in chemical reaction parameter(γ) enhances τx and reduces τz on the wall in both degenerating and generating chemical reaction cases. Both skin friction components τx,τz and Nu enhances with suction parameter(fw>0) and reduces with that of (fw<0) on the wall. The effect of Prandtl number is to reduce the skin friction, Sherwood number and enhance the Nusselt number.

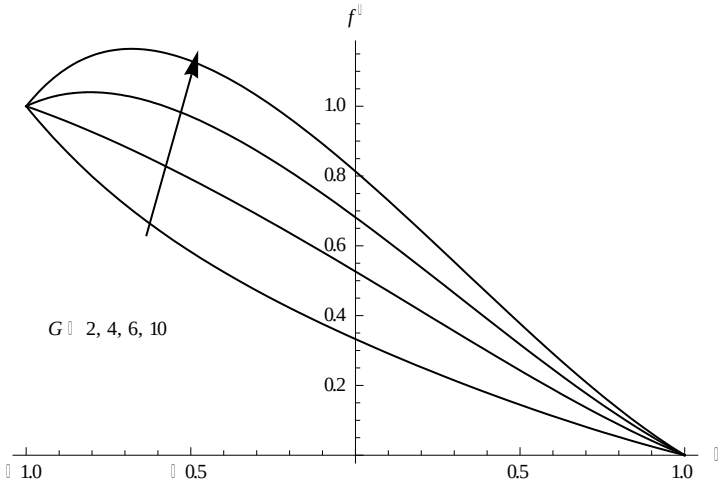

Fig.2a: Variation of Primary velocity(f') with G
M=0.5, Nr=0.5, N=1.0, A11=0.1, B11=0.1, Ec=0.01, R=0.5, Pr=0.71, Nb=0.1, Nt=0.1

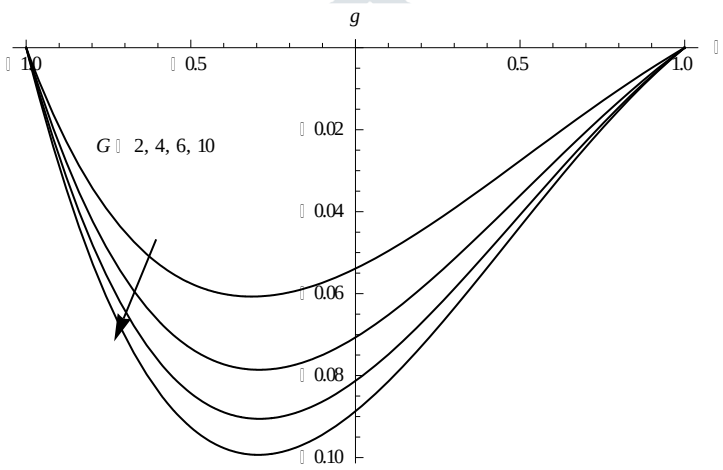

Fig.2b:Variation of secondary velocity(g) with G
M=0.5, Nr=0.5, N=1.0, A11=0.1, B11=0.1, Ec=0.01, R=0.5, Pr=0.71, Nb=0.1, Nt=0.1

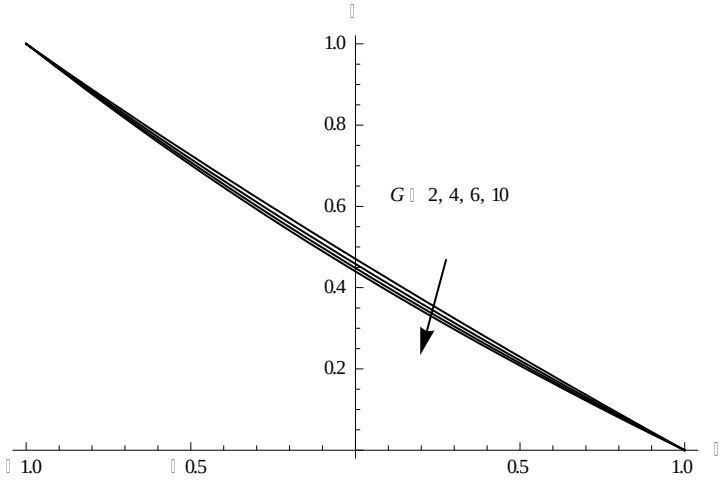

Fig.2c : Variation of Temperature(θ) with G
M=0.5, Nr=0.5, N=1.0, A11=0.1, B11=0.1, Ec=0.01, R=0.5, Pr=0.71, Nb=0.1, Nt=0.1

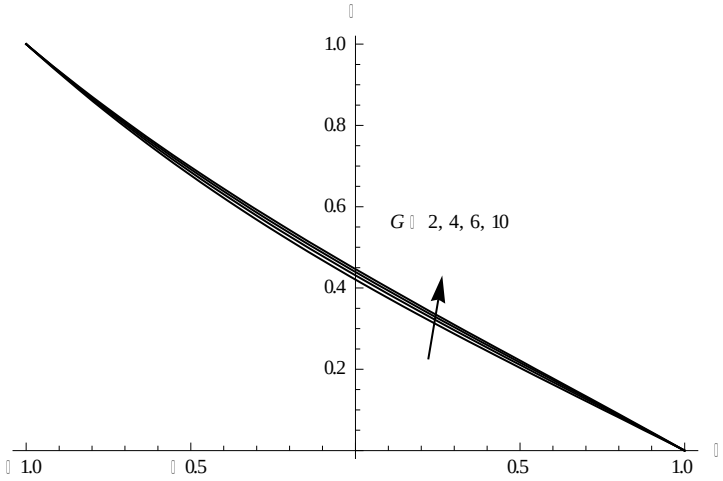

Fig.2d :Variation of Nano concentration(ϕ) with G
M=0.5, Nr=0.5, N=1.0, A11=0.1, B11=0.1, Ec=0.01, R=0.5, Pr=0.71, Nb=0.1, Nt=0.1

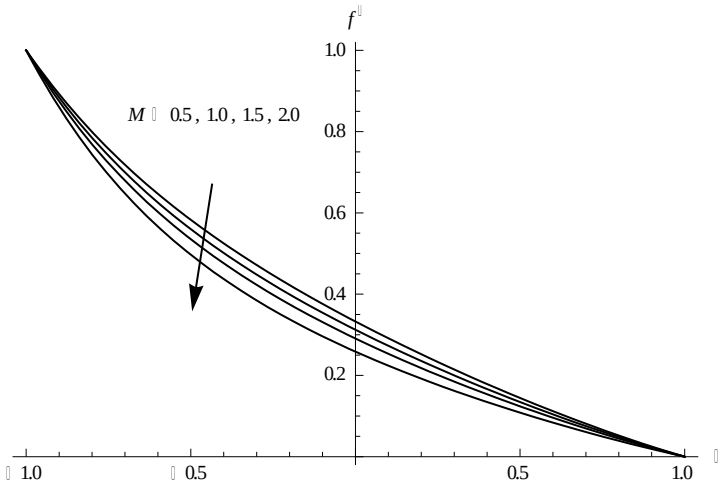

Fig.3a:Variation of Primary velocity(f') with M
G=2, Nr=0.5, N=1.0, A11=0.1, B11=0.1, Ec=0.01, R=0.5, Nb=0.1, Nt=0.1

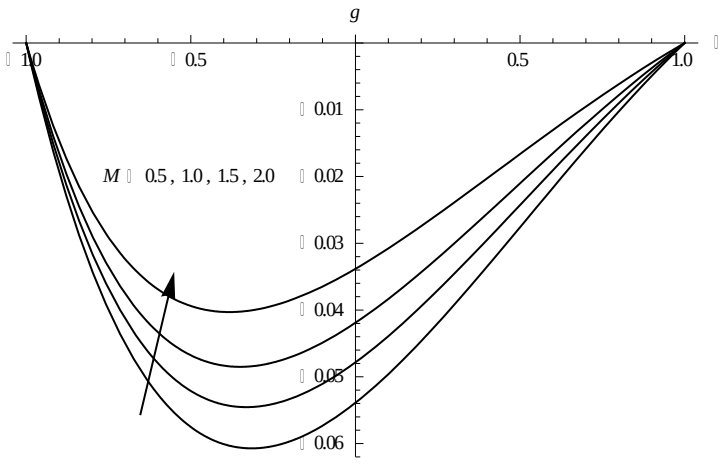

Fig.3b:Variation of secondary velocity(g) with M
G=2, Nr=0.5, N=1.0, A11=0.1, B11=0.1, Ec=0.01, R=0.5, Pr=0.71, Nb=0.1, Nt=0.1

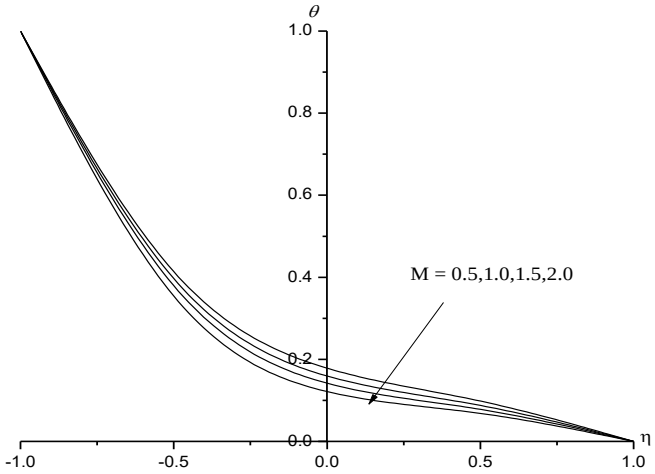

Fig.3c: Variation of temperature(θ) with M
G=2, Nr=0.5, N=1.0, A11=0.1, B11=0.1, Ec=0.01, R=0.5, Pr=0.71, Nb=0.1, Nt=0.1

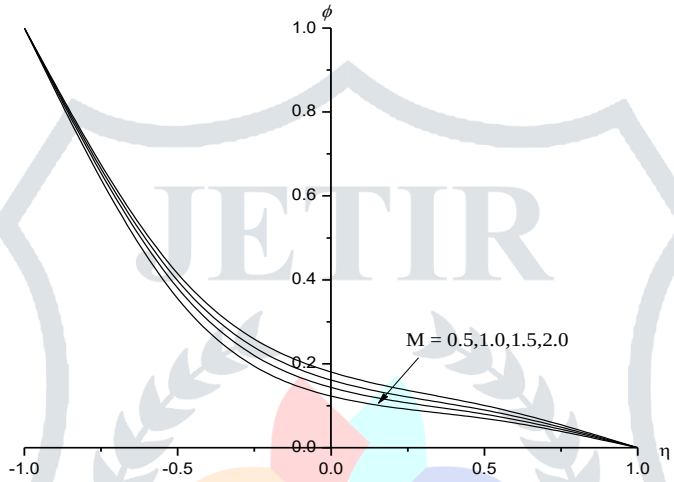

Fig.3d : Variation of Nano concentration(ϕ) with M
G=2, Nr=0.5, N=1.0, A11=0.1, B11=0.1, Ec=0.01, R=0.5, Pr=0.71, Nb=0.1, Nt=0.1

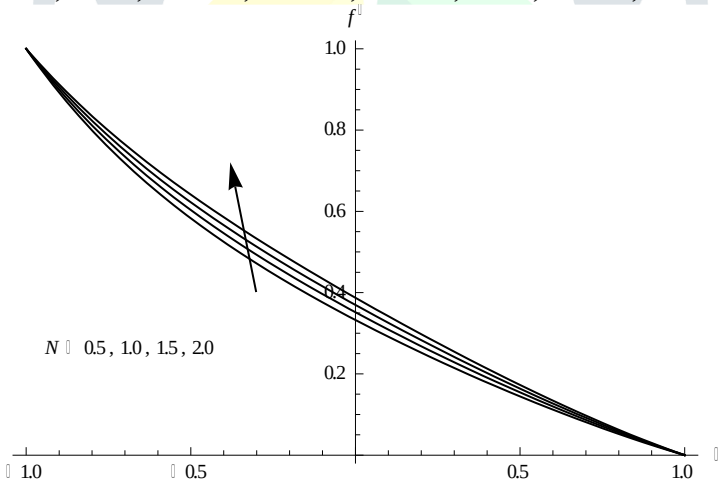

Fig.4a:Variation of Primary velocity(f') with N
M=0.5, Nr=0.5, G=2, A11=0.1, B11=0.1, Ec=0.01, R=0.5, Nb=0.1, Nt=0.1

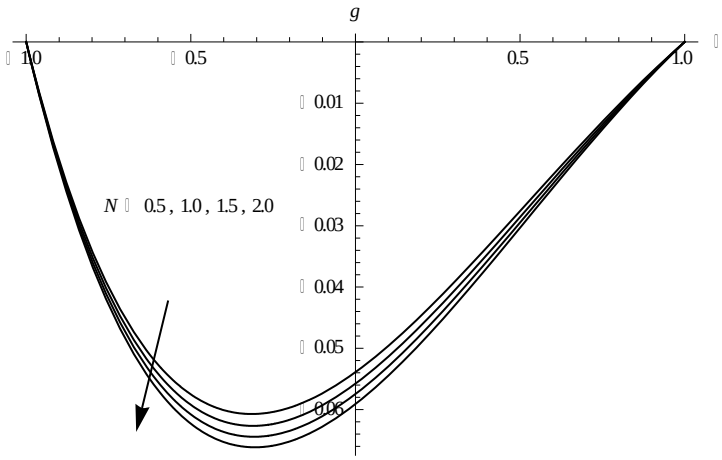

Fig.4b:Variation of secondary velocity(g) with N
M=0.5, Nr=0.5, N=1.0, A11=0.1, B11=0.1, Ec=0.01, R=0.5, Nb=0.1, Nt=0.1

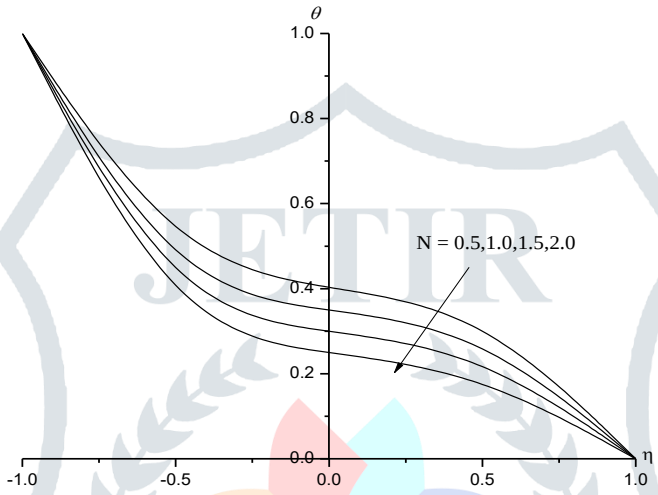

Fig.4c: Variation of temperature(θ) with N
M=0.5, Nr=0.5, G=2, A11=0.1, B11=0.1, Ec=0.01, Nb=0.1, Nt=0.1

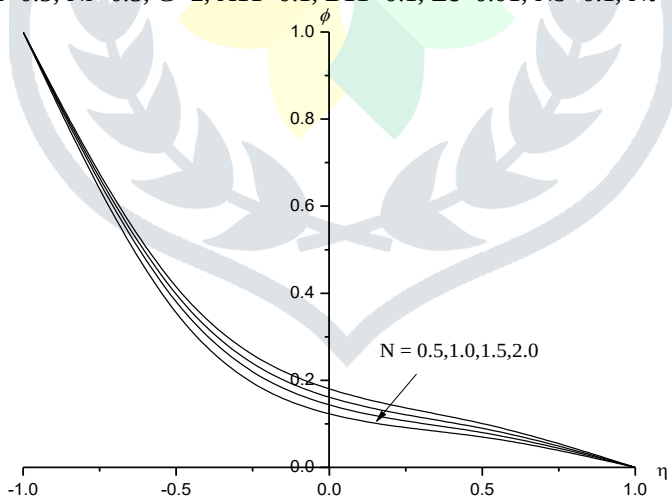

Fig.4d: Variation of Nano concentration(ϕ) with N
M=0.5, Nr=0.5, G=2, A11=0.1, B11=0.1, Ec=0.01, R=0.5, Nb=0.1, Nt=0.1

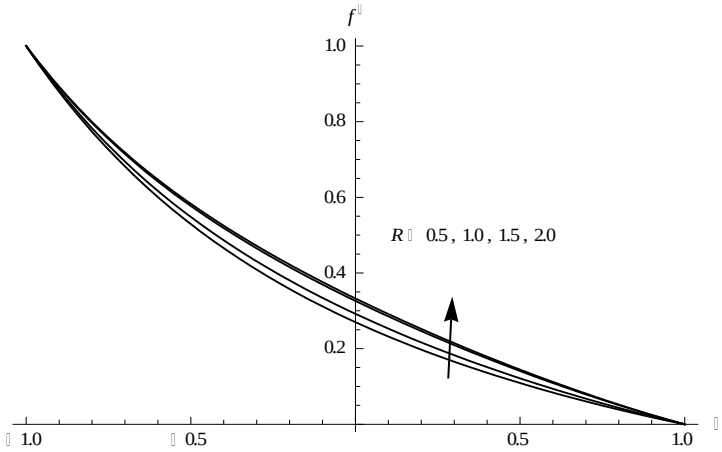

Fig.5a:Variation of Primary velocity(f') with R

M=0.5, Nr=0.5, G=2, A11=0.1, B11=0.1, Ec=0.01, N=1, Nb=0.1, Nt=0.1

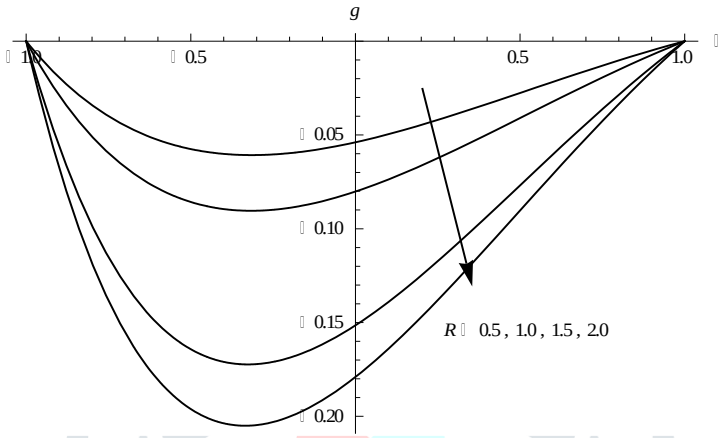

Fig.5b: Variation of Secondary velocity(g) with R

M=0.5, Nr=0.5, G=2, A11=0.1, B11=0.1, Ec=0.01, N=1, Nb=0.1, Nt=0.1

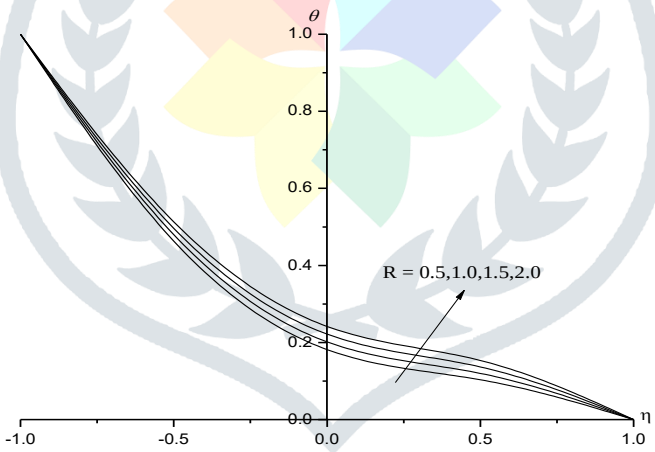

Fig.5c: Variation of Temperature(θ) with R

M=0.5, Nr=0.5, N=1.0, A11=0.1, B11=0.1, Ec=0.01, N=1, Nb=0.1, Nt=0.1

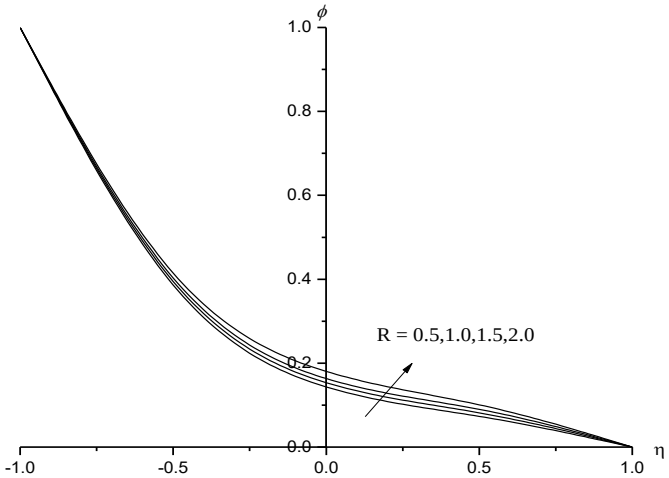

Fig.5d : Variation of Nano concentration(ϕ) with R

M=0.5, Nr=0.5, N=1.0, A11=0.1, B11=0.1, Ec=0.01, N=1, Nb=0.1, Nt=0.1

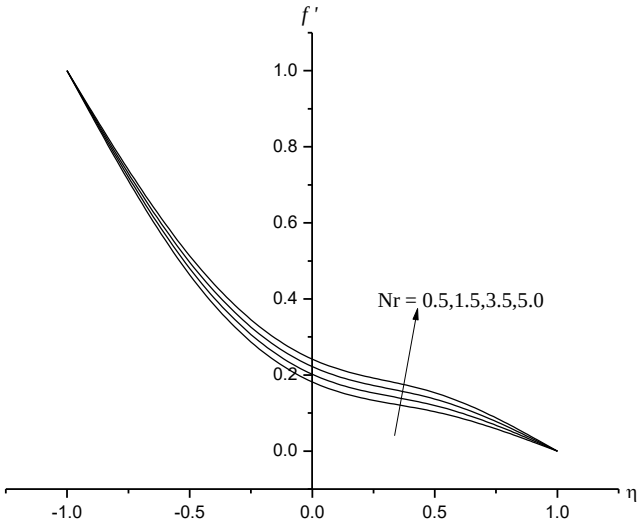

Fig.6a:Variation of Primary velocity(f') with Nr
M=0.5, Nr=0.5, N=1.0, A11=0.1, B11=0.1, Ec=0.01, R=0.5, Nb=0.1, Nt=0.1

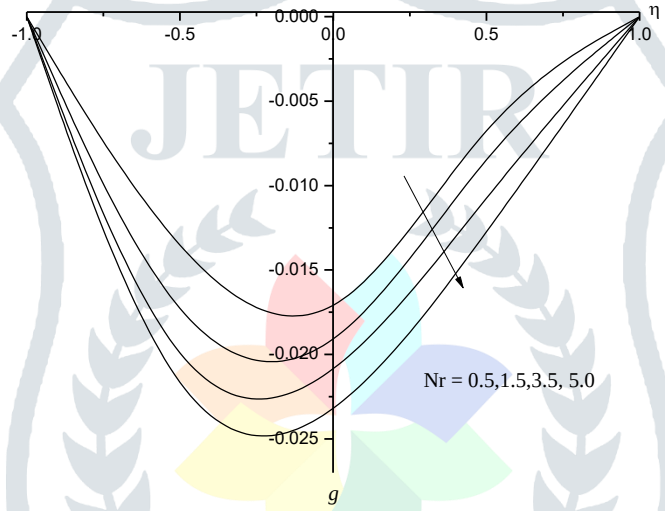

Fig.6b:Variation of secondary velocity(g) with Nr
M=0.5, Nr=0.5, N=1.0, A11=0.1, B11=0.1, Ec=0.01, R=0.5, Nb=0.1, Nt=0.1

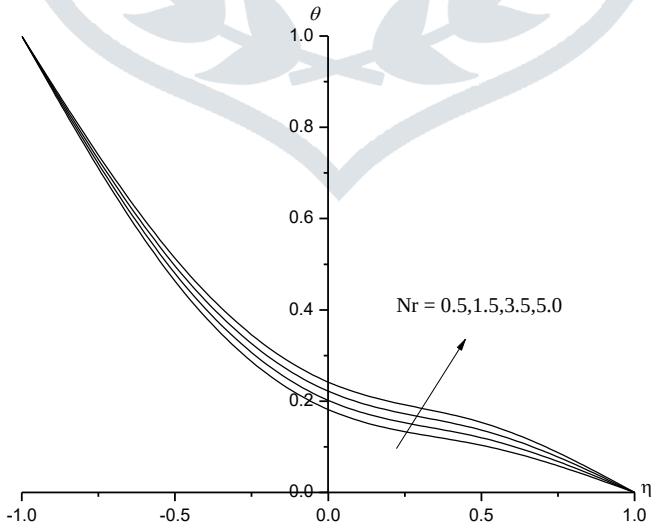

Fig.6c: Variation of temperature(θ) with Nr
M=0.5, Nr=0.5, N=1.0, A11=0.1, B11=0.1, Ec=0.01, R=0.5, Nb=0.1, Nt=0.1

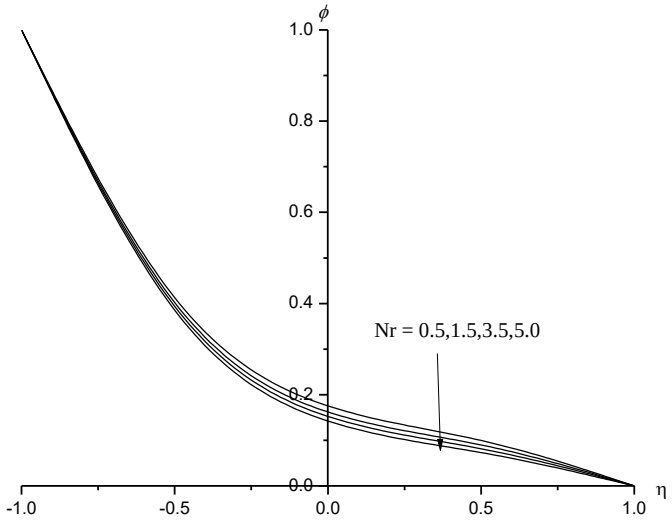

Fig.6d: Variation of Nano concentration(ϕ) with Nr
M=0.5, Nr=0.5, N=1.0, A11=0.1, B11=0.1, Ec=0.01, R=0.5, Nb=0.1, Nt=0.1

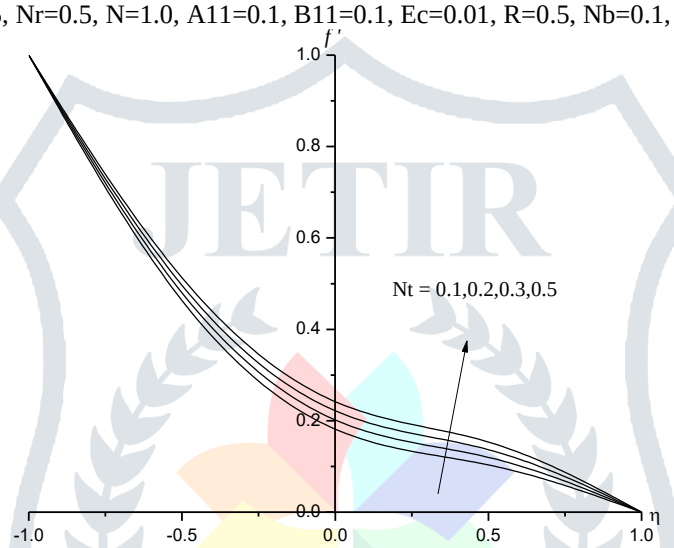

Fig.7a:Variation of Primary velocity(f') with Nt
M=0.5, Nr=0.5, N=1.0, A11=0.1, B11=0.1, Ec=0.01, R=0.5, Nb=0.1, Nt=0.1

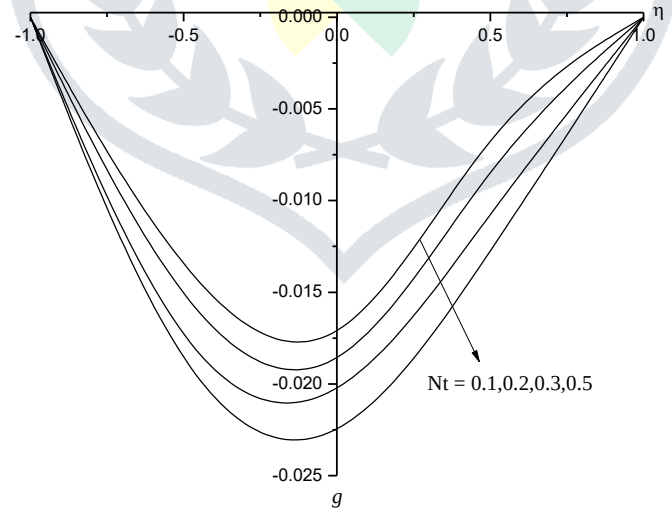

Fig.7b:Variation of secondary velocity(g) with Nt
M=0.5, Nr=0.5, N=1.0, A11=0.1, B11=0.1, Ec=0.01, R=0.5, Nb=0.1

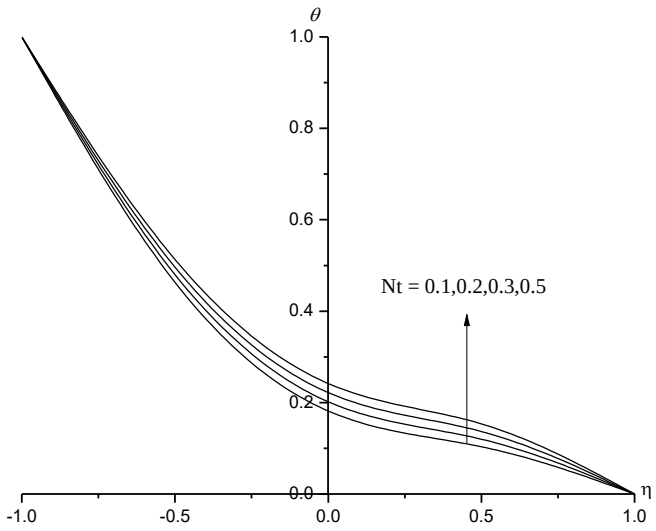

Fig.7c :Variation of temperature(θ) with Nt
M=0.5, Nr=0.5, N=1.0, A11=0.1, B11=0.1, Ec=0.01, R=0.5, Nb=0.1

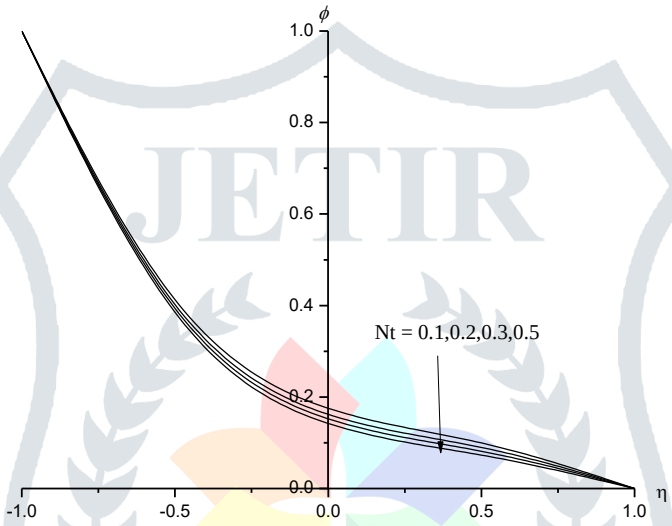

Fig.7d: Variation of Nano concentration(ϕ) with Nt
M=0.5, Nr=0.5, N=1.0, A11=0.1, B11=0.1, Ec=0.01, R=0.5, Nb=0.1

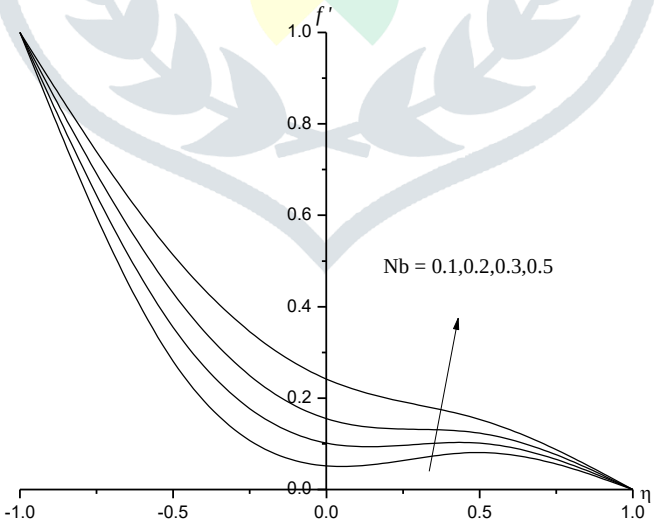

Fig.8a: Variation of Primary velocity(f') with Nb
M=0.5, Nr=0.5, N=1.0, A11=0.1, B11=0.1, Ec=0.01, R=0.5, Nt=0.1

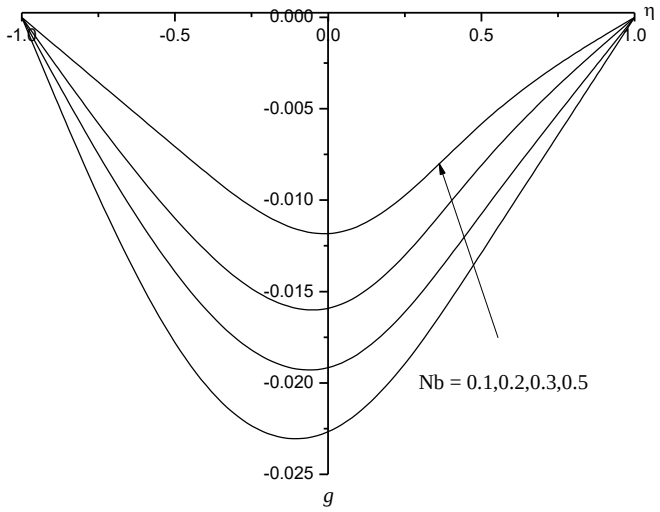

Fig.8b: Variation of secondary velocity(g) with Nb
M=0.5, Nr=0.5, N=1.0, A11=0.1, B11=0.1, Ec=0.01, R=0.5, Nt=0.1

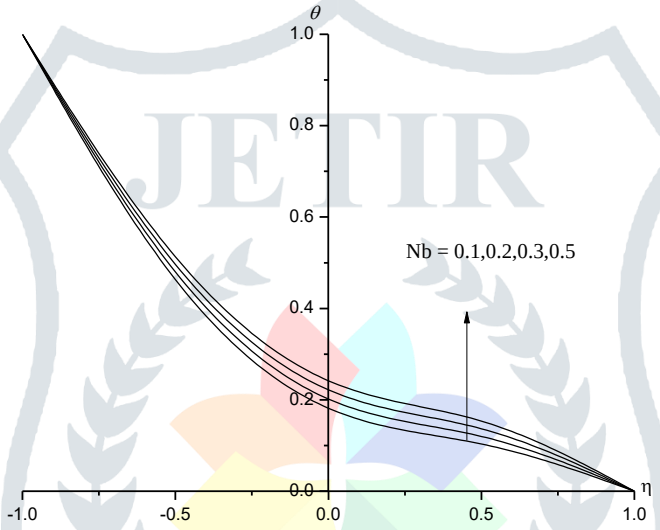

Fig.8c: Variation of temperature(θ) with Nb
M=0.5, Nr=0.5, N=1.0, A11=0.1, B11=0.1, Ec=0.01, R=0.5, Nt=0.1

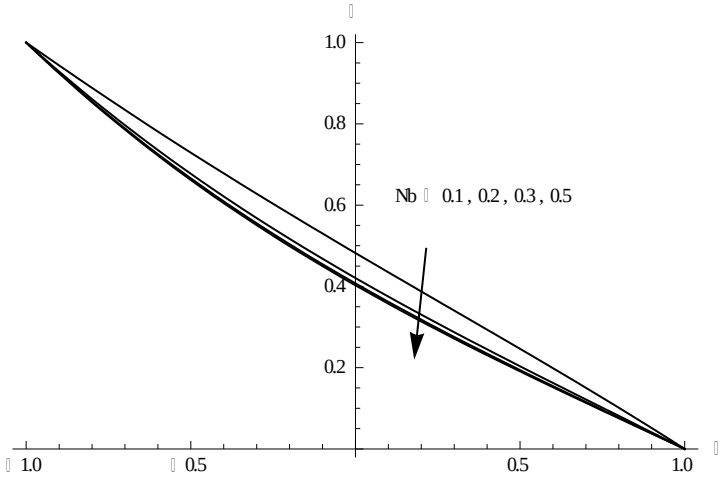

Fig.8d: Variation of Nano concentration (ϕ) with Nt
M=0.5, Nr=0.5, N=1.0, A11=0.1, B11=0.1, Ec=0.01, R=0.5, Nt=0.1

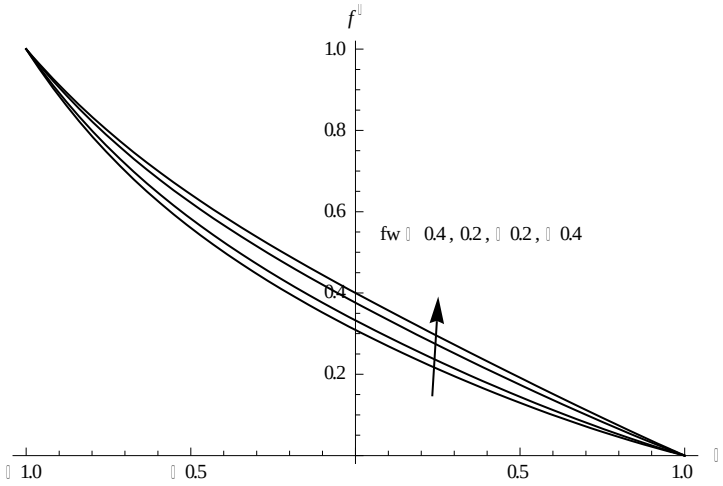

Fig.9a: Variation of Primary velocity(f') with fw
M=0.5, Nr=0.5, N=1.0, A11=0.1, B11=0.1, Ec=0.01, R=0.5, Nb=0.1, Nt=0.1

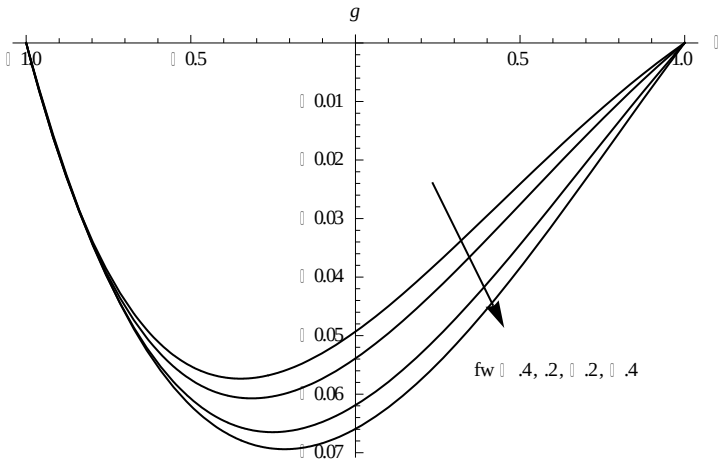

Fig.9b: Variation of secondary velocity(g) with fw
M=0.5, Nr=0.5, N=1.0, A11=0.1, B11=0.1, Ec=0.01, R=0.5, Nb=0.1, Nt=0.1

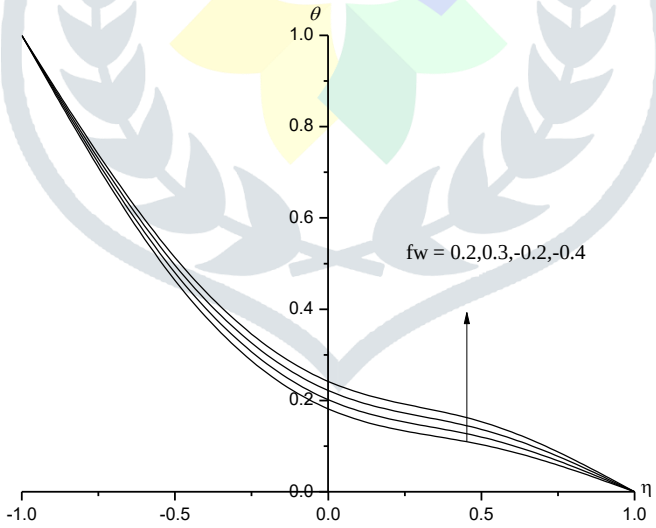

Fig.9c : Variation of temperature(θ) with fw
M=0.5, Nr=0.5, N=1.0, A11=0.1, B11=0.1, Ec=0.01, R=0.5, Nb=0.1, Nt=0.1

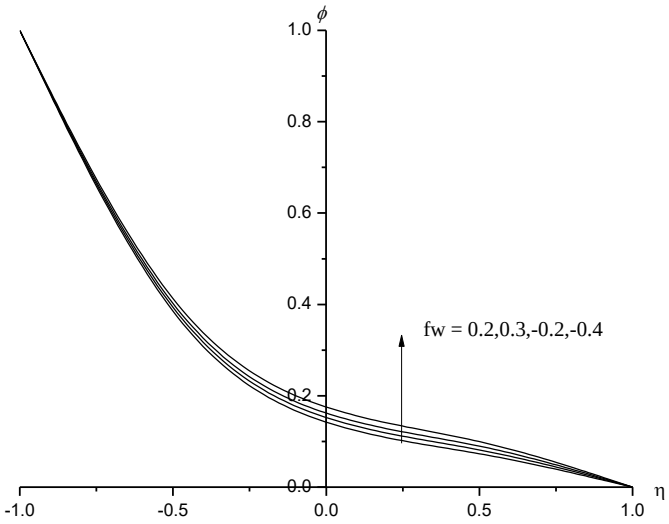

Fig.9d: Variation of Nano concentration(ϕ) with fw

M=0.5, Nr=0.5, N=1.0, A11=0.1, B11=0.1, Ec=0.01, R=0.5, Nb=0.1, Nt=0.1

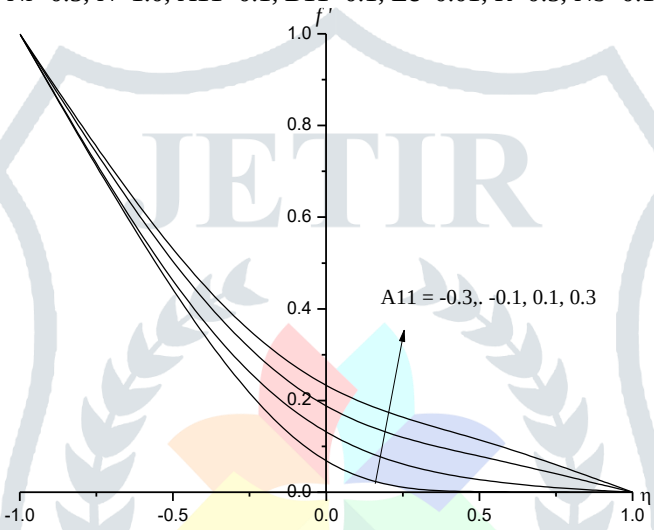

Fig.10a: Variation of Primary velocity(f') with A11

G=2, M=0.5, Nr=0.5, N=1.0, fw=0.2, B11=0.1, Ec=0.01, R=0.5, Nb=0.1, Nt=0.1

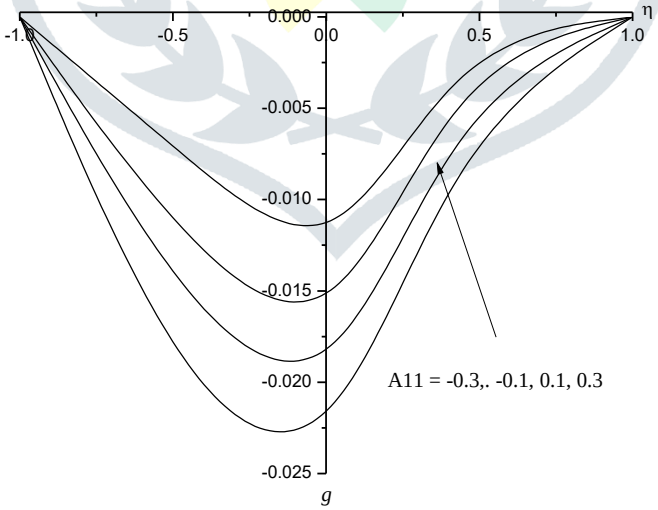

Fig.10b:Variation of secondary velocity(g) with A11

M=0.5, Nr=0.5, N=1.0, G=2, fw=0.2, B11=0.1, Ec=0.01, R=0.5, Nb=0.1, Nt=0.1

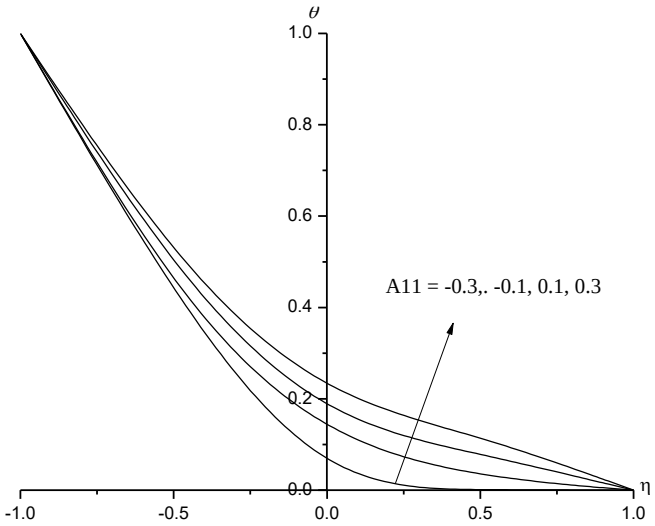

Fig.10c: Variation of Temperature(θ) with A11
M=0.5, Nr=0.5, N=1.0, G=2, fw=0.2, B11=0.1, Ec=0.01, R=0.5, Nb=0.1, Nt=0.1

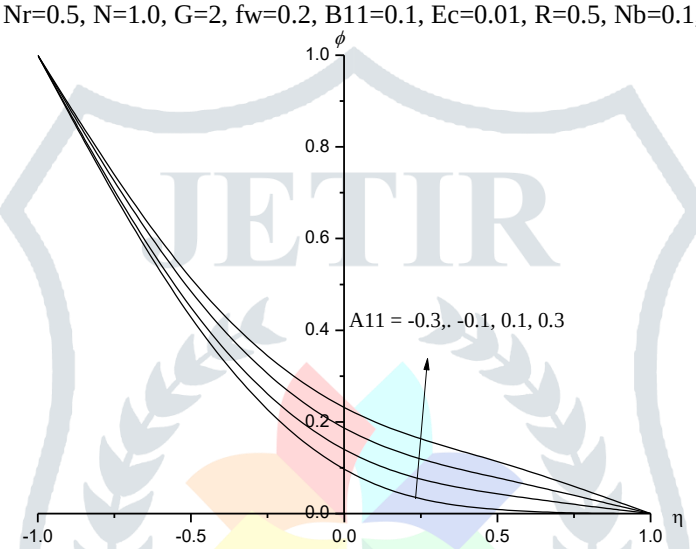

Fig.10d : Variation of Nano concentration(ϕ) with A11
M=0.5, Nr=0.5, N=1.0, G=2, fw=0.2, B11=0.1, Ec=0.01, R=0.5, Nb=0.1, Nt=0.1

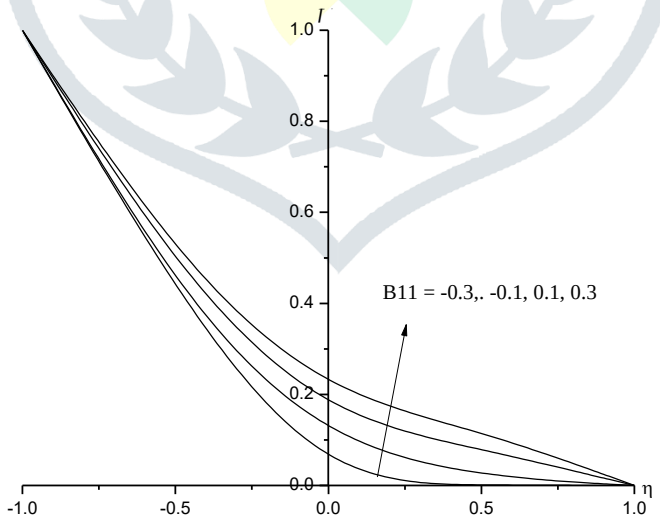

Fig.11a:Variation of Primary velocity(f') with B11
M=0.5, Nr=0.5, N=1.0, G=2, A11=0.1, Ec=0.01, R=0.5, Nb=0.1, Nt=0.1

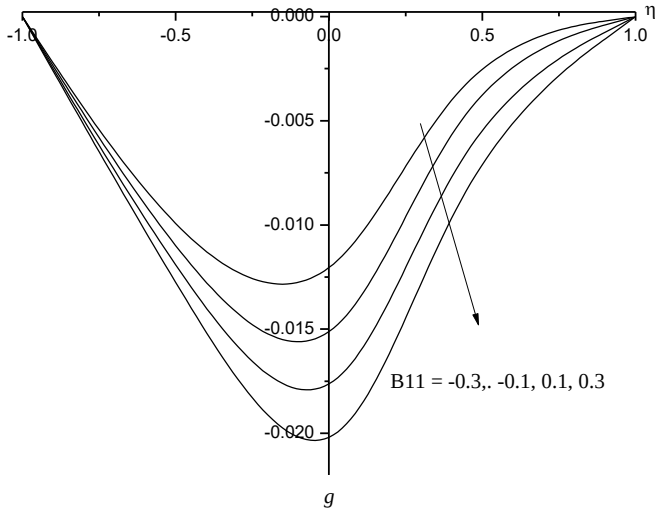

Fig.11b:Variation of Secondary velocity(g) with B11
M=0.5, Nr=0.5, N=1.0, A11=0.1, G=2, Ec=0.01, R=0.5, Nb=0.1, Nt=0.1

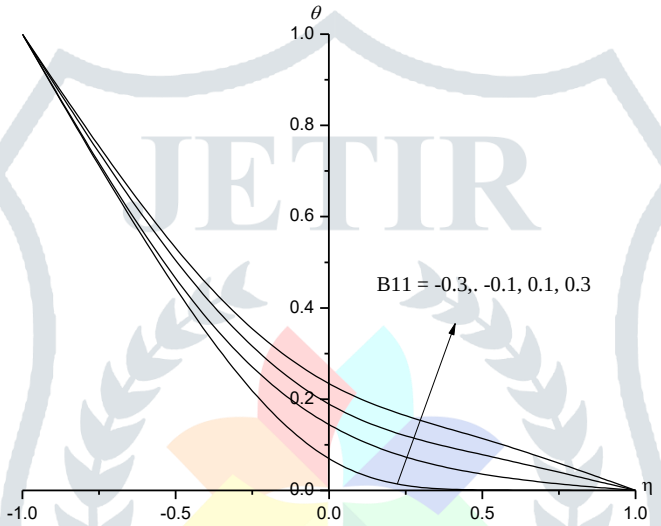

Fig.11c :Variation of Temperature(θ) with B11
M=0.5, Nr=0.5, N=1.0, A11=0.1, G=2, Ec=0.01, R=0.5, Nb=0.1, Nt=0.1

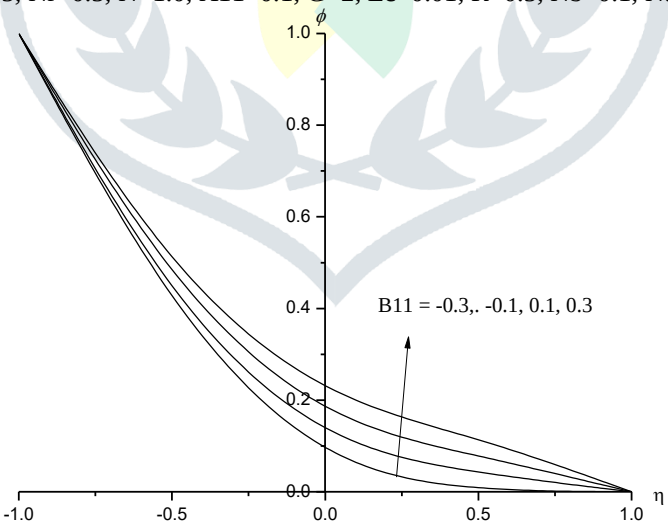

Fig.11d :Variation of Nano concentration(ϕ) with B11
M=0.5, Nr=0.5, N=1.0, A11=0.1, G=2, Ec=0.01, R=0.5, Nb=0.1, Nt=0.1

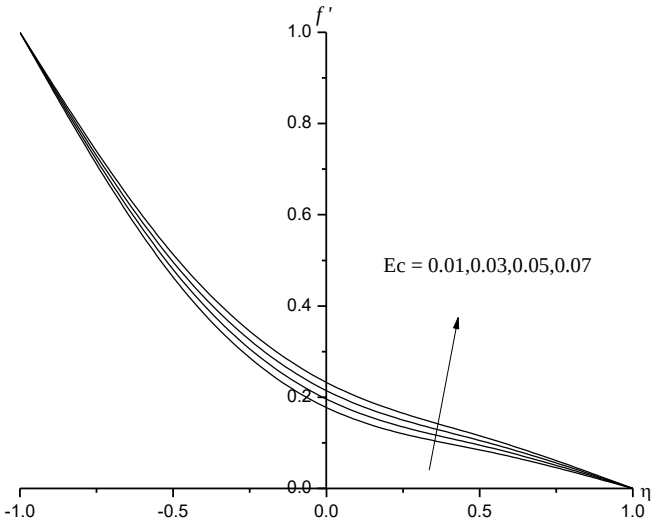

Fig.12a: Variation of Primary velocity(f') with Ec
M=0.5, Nr=0.5, N=1.0, A11=0.1, B11=0.1, R=0.5, G=2, Nb=0.1, Nt=0.1

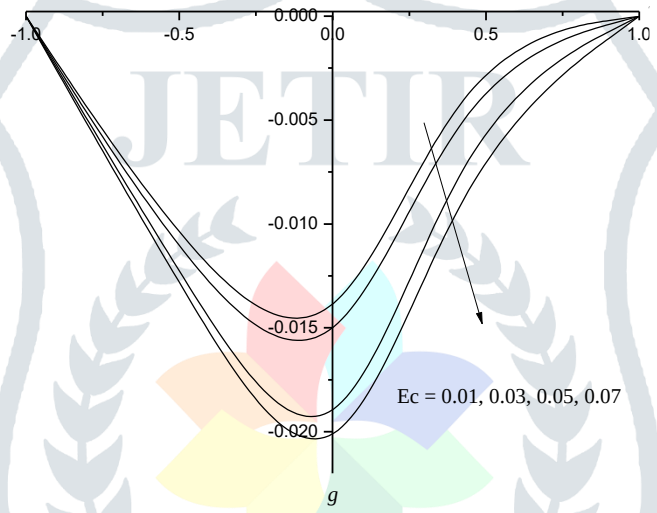

Fig.12b:Variation of Secondary velocity(g) with Ec
M=0.5, Nr=0.5, N=1.0, A11=0.1, B11=0.1, R=0.5, G=2, Nb=0.1, Nt=0.1

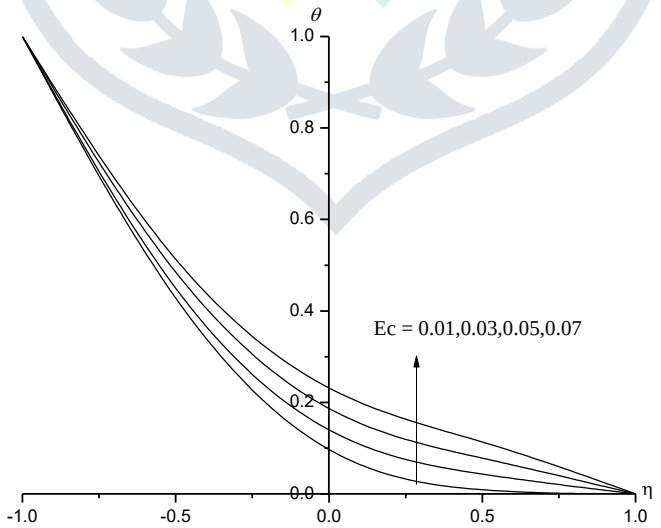

Fig.12c: Variation of Temperature(θ) with Ec
M=0.5, Nr=0.5, N=1.0, A11=0.1, B11=0.1, R=0.5, G=2, Nb=0.1, Nt=0.1

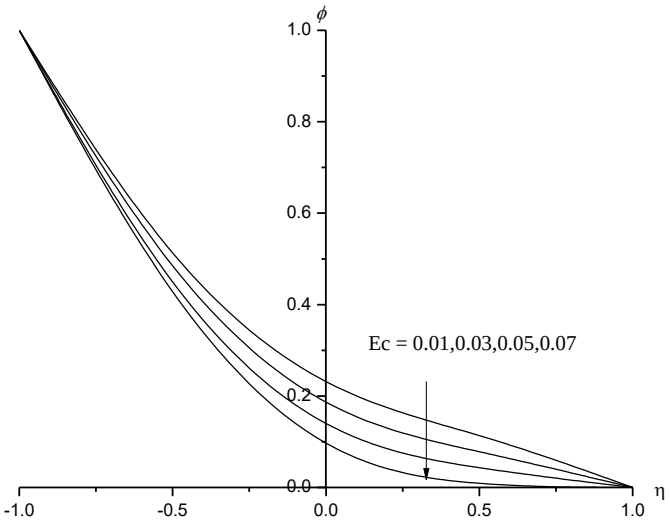

Fig.12d: Variation of Nano concentration(ϕ) with Ec
M=0.5, Nr=0.5, N=1.0, A11=0.1, B11=0.1, R=0.5, G=2, Nb=0.1, Nt=0.1

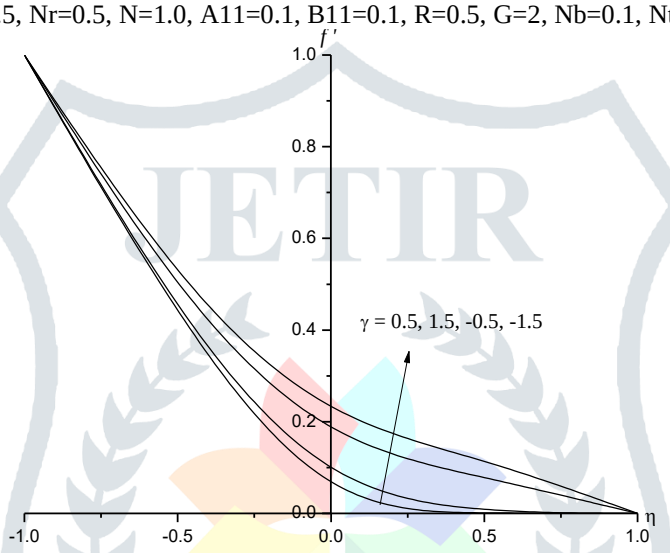

Fig.13a: Variation of Primary velocity(f') with γ
M=0.5, Nr=0.5, N=1.0, A11=0.1, B11=0.1, R=0.5, G=2, Nb=0.1, Nt=0.1

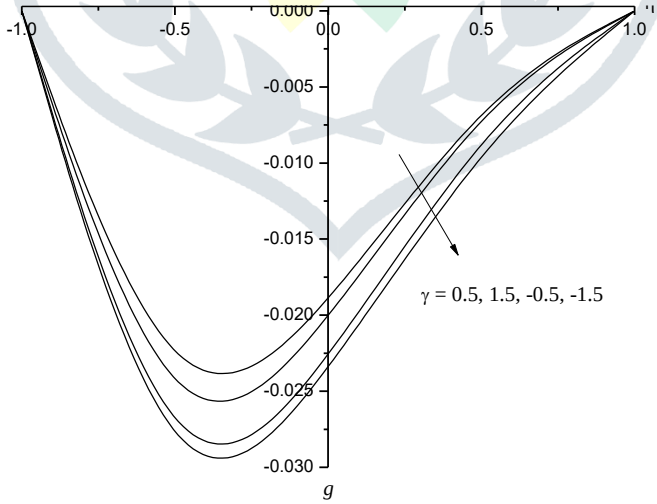

Fig.13b: Variation of Secondary velocity(g) with γ
M=0.5, Nr=0.5, N=1.0, A11=0.1, B11=0.1, R=0.5, G=2, Nb=0.1, Nt=0.1

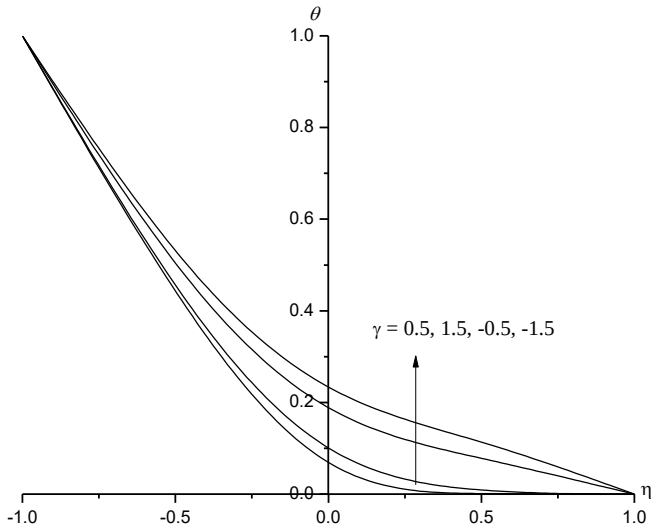

Fig.13c: Variation of temperature(θ) with γ
M=0.5, Nr=0.5, N=1.0, A11=0.1, B11=0.1, R=0.5, G=2, Nb=0.1, Nt=0.1

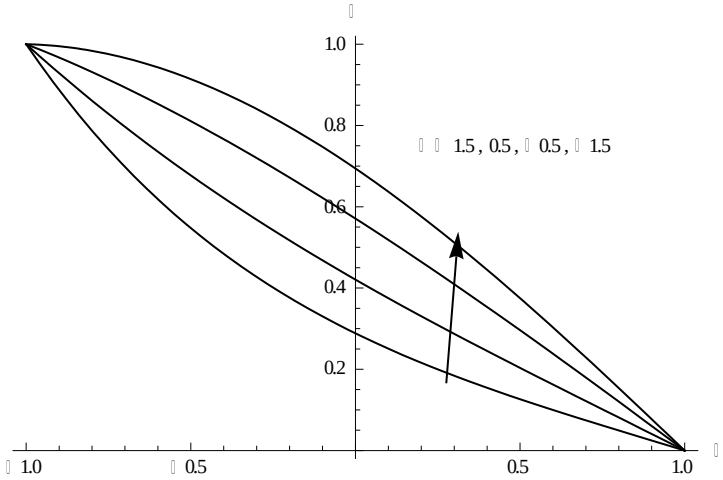

Fig.13d: Variation of Nano concentration(ϕ) with γ
M=0.5, Nr=0.5, N=1.0, A11=0.1, B11=0.1, R=0.5, G=2, Nb=0.1, Nt=0.1

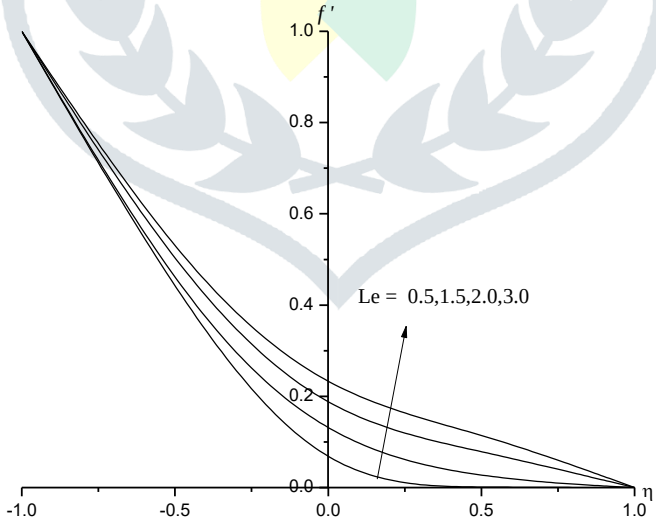

Fig.14a: Variation of Primary velocity(f') with Le
M=0.5, Nr=0.5, N=1.0, A11=0.1, B11=0.1, G=2, R=0.5, Nb=0.1, Nt=0.1

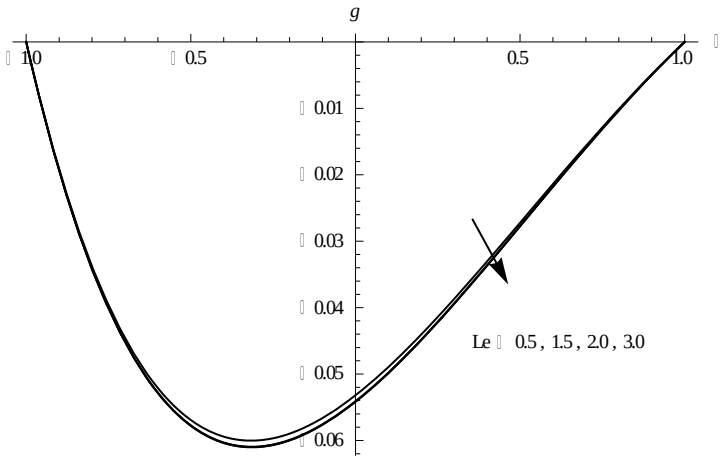

Fig.14b: Variation of secondary velocity(g) with Le
M=0.5, Nr=0.5, N=1.0, A11=0.1, B11=0.1, r=0.5, G=2, Nb=0.1, Nt=0.1

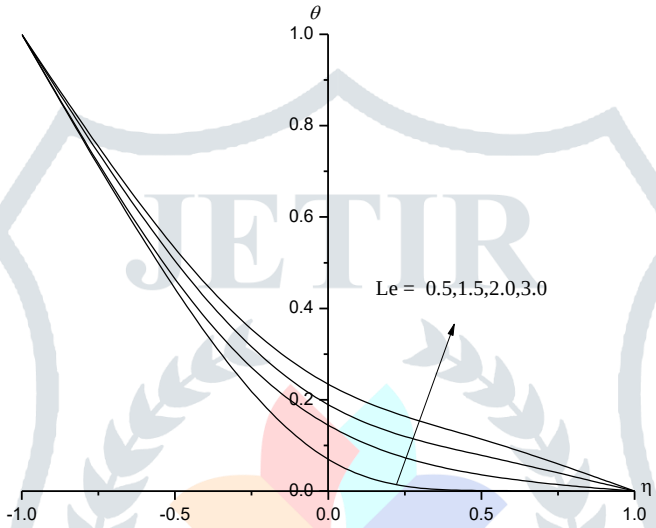

Fig.14c: Variation of temperature(θ) with Le
M=0.5, Nr=0.5, N=1.0, A11=0.1, B11=0.1, R=0.5, G=2,Nb=0.1, Nt=0.1

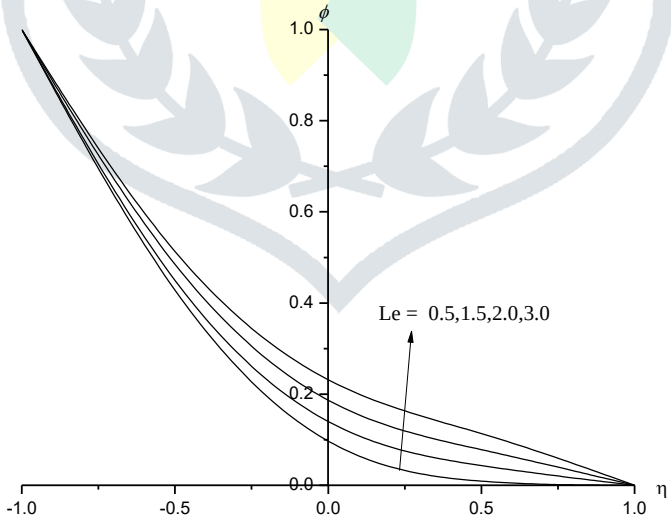

Fig.14d: Variation of Nanoconcentration(ϕ) with Le
M=0.5, Nr=0.5, N=1.0, A11=0.1, B11=0.1, r=0.5, G=2, Nb=0.1, Nt=0.1

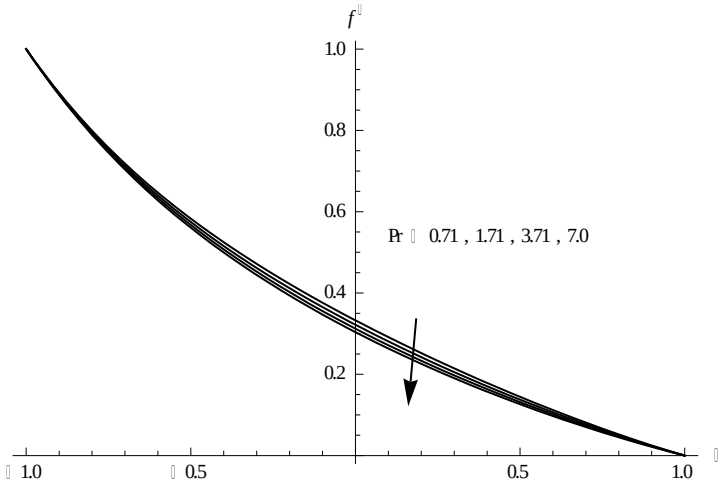

Fig.15a: Variation of Primary velocity(f') with Pr
M=0.5, Nr=0.5, N=1.0, A11=0.1, B11=0.1, R=0.5, G=2, Nb=0.1, Nt=0.1

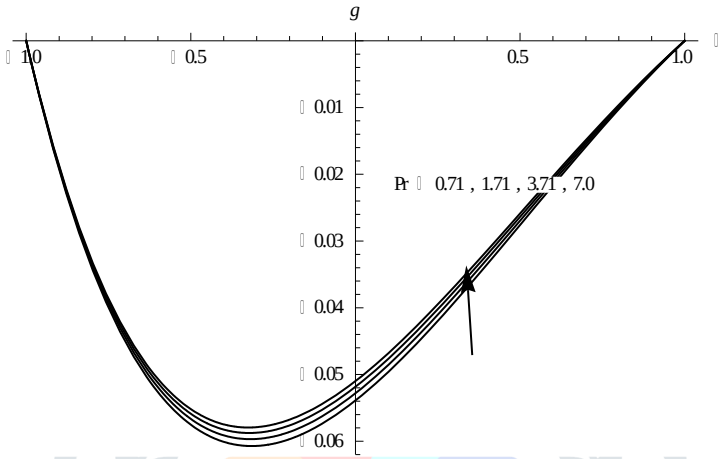

Fig.15b: Variation of secondary velocity(g) with Pr
M=0.5, Nr=0.5, N=1.0, A11=0.1, B11=0.1, Ec=0.01, Nb=0.1, Nt=0.1

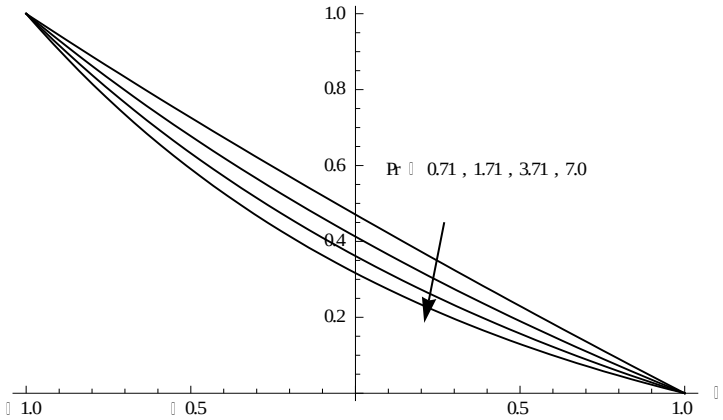

Fig.15c : Variation of temperature(θ) with Pr
M=0.5, Nr=0.5, N=1.0, A11=0.1, B11=0.1, R=0.5, G=2, Nb=0.1, Nt=0.1

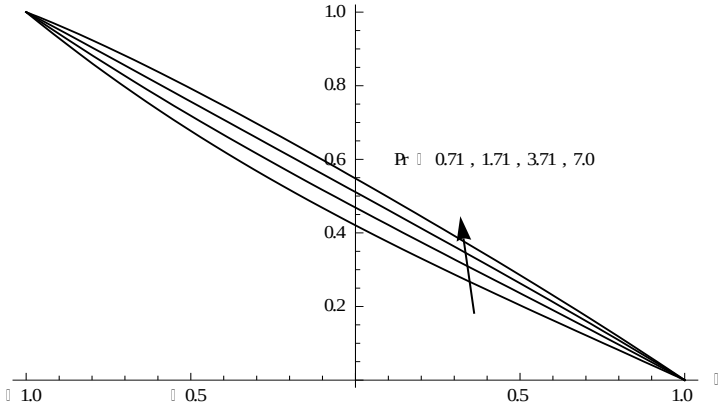

Fig.15d: Variation of Nano concentration(ϕ) with Pr
M=0.5, Nr=0.5, N=1.0, A11=0.1, B11=0.1, R=0.5, G=2, Nb=0.1, Nt=0.1

Table 1: Skin friction, ($\tau_{x,z}$), Nusselt number(Nu) and Sherwood number (Sh) at η=–1

Parameter		τx(-1)	τz(-1)	Nu(-1)	Sh(-1)
G	2	-1.16703	-0.21899	0.572923	0.731538
	4	-0.736352	-0.242222	0.585048	0.721255
	6	-0.326783	-0.261528	0.595853	0.71208
	10	-0.0663102	-0.278096	0.605656	0.703747
M	0.5	-1.16001	-0.22003	0.573119	0.73137
	1	-1.2653	-0.205156	0.570211	0.733856
	1.5	-1.76374	-0.152015	0.557491	0.744761
	2	-1.99979	-0.135145	0.551985	0.749494
N	1	-1.16703	-0.21899	0.572923	0.731538
	2	-1.0864	-0.223477	0.575197	0.729609
	-0.5	-1.01015	-0.227617	0.577326	0.727803
	-1.5	-0.934395	-0.231637	0.57942	0.726026
R	0.5	-1.16703	-0.21899	0.572923	0.731538
	1	-1.1812	-0.327091	0.572282	0.732076
	1.5	-1.25465	-0.636413	0.568952	0.73487
	2	-1.30236	-0.7692	0.566787	0.736687
Nr	0..5	-1.16001	-0.22003	0.573119	0.73137
	1.5	-1.15768	-0.220275	0.554481	0.747941
	3.5	-1.15582	-0.22047	0.539719	0.76106
	5	-1.14866	-0.238703	0.527162	0.772191
γ	0.5	-1.16001	-0.22003	0.573119	0.73137
	1.5	-1.16527	-0.219497	0.569243	1.19322
	-0.5	-1.15454	-0.220612	0.57736	0.315125
	-1.5	-1.19397	-0.218175	0.579322	0.0197983
Nb	0.1	-1.15971	-0.220062	0.586746	0.566106
	0.2	-1.16001	-0.220083	0.573119	0.73137
	0.3	-1.17854	-0.220189	0.559834	0.764232
	0.5	-1.19167	-0.238466	0.545866	0.77855

Parameter		τx(-1)	τz(-1)	Nu(-1)	Sh(-1)
Nt	0.1	-1.16354	-0.219646	0.598622	0.709005
	0.2	-1.15971	-0.220062	0.586746	0.566106
	0.3	-1.15651	-0.220407	0.57504	0.463665
	0.5	-1.1425	-0.238318	0.562333	0.407595
fw	0.2	-1.16001	-0.22003	0.573119	0.73137
	0.4	-1.24421	-0.22174	0.587431	0.718922
	-0.2	-1.00977	-0.213932	0.545253	0.755534
	-0.4	-0.973588	-0.208196	0.530792	0.768013
Ec	0.01	-1.16001	-0.22003	0.573119	0.73137
	0.03	-1.15985	-0.220046	0.571438	0.732913
	0.05	-1.1597	-0.220061	0.569758	0.734455
	0.07	-1.4428	-0.238105	0.566975	0.736955
A11	0.1	-1.16001	-0.22003	0.573119	0.73137
	0.3	-1.15942	-0.22009	0.567993	0.735977
	-0.1	-1.1606	-0.219971	0.578242	0.726767
	-0.3	-1.19606	-0.217925	0.582244	0.723113
B11	0.1	-1.16354	-0.219646	0.598622	0.709005
	0.3	-1.16279	-0.219724	0.592428	0.714531
	-0.1	-1.1643	-0.219569	0.604786	0.703504
	-0.3	-1.20033	-0.217457	0.610214	0.698617
Le	1.0	-1.16354	-0.219646	0.598622	0.709005
	2.0	-1.1639	-0.219724	0.59992	0.70531
	3.0	-1.16434	-0.21999	0.604786	0.70504
	4.0	-1.20033	-0.22457	0.610214	0.698617
Pr	0.71	-1.16001	-0.22003	0.573119	0.73137
	1.71	-1.17947	-0.21794	0.722155	0.599516
	3.71	-1.1972	-0.216062	0.865775	0.471376
	7.00	-1.25243	-0.211881	0.999349	0.351101

Table 2: Skin friction, ($\tau_{x,z}$), Nusselt number(Nu) and Sherwood number (Sh) at η=+1

Parameter		τx(+1)	τz(+1)	Nu(+1)	Sh(+1)
G	2	-0.238377	0.047153	0.447996	0.409522
	4	-0.324246	0.054395	0.436193	0.419533
	6	-0.393204	0.0590561	0.425945	0.428208
	10	-0.450282	0.0621197	0.416848	0.435894
M	0.5	-0.239542	0.047573	0.447817	0.409673
	1	-0.222416	0.0416007	0.450465	0.407431
	1.5	-0.152835	0.0214176	0.46183	0.397803
	2	-0.124507	0.0156673	0.466687	0.393686
N	1	-0.238377	0.047153	0.447996	0.409522
	2	-0.254792	0.0486616	0.445774	0.411408
	-0.5	-0.269931	0.0499988	0.443702	0.413166
	-1.5	-0.284617	0.0512466	0.441672	0.414888
R	0.5	-0.238377	0.047153	0.447996	0.409522
	1	-0.23205	0.0700743	0.448688	0.408933
	1.5	-0.199061	0.131879	0.452288	0.405867
	2	-0.177568	0.155183	0.454631	0.403871
Nr	0.5	-0.239542	0.047573	0.447817	0.409673
	1.5	-0.240991	0.047695	0.458234	0.40107
	3.5	-0.242144	0.0477918	0.46657	0.394178
	5	-0.23615	0.0472169	0.474	0.388014
γ	0.5	-0.239542	0.047573	0.447817	0.409673
	1.5	-0.236546	0.0473156	0.445262	0.249667
	-0.5	-0.243015	0.0478649	0.450639	0.606102
	-1.5	-0.233354	0.0469691	0.454403	0.772858
Nb	0.1	-0.239753	0.0475896	0.438682	0.521245
	0.2	-0.239542	0.047573	0.447817	0.409673
	0.3	-0.240522	0.0476542	0.456963	0.387345
	0.5	-0.234873	0.047104	0.46717	0.377383

Parameter		τx(+1)	τz(+1)	Nu(+1)	Sh(+1)
Nt	0.1	-0.237115	0.047373	0.428597	0.425952
	0.2	-0.239753	0.0475896	0.438682	0.521245
	0.3	-0.241941	0.0477686	0.448989	0.581115
	0.5	-0.234104	0.0470354	0.460732	0.59707
fw	0.2	-0.239542	0.047573	0.447817	0.409673
	0.4	-0.209144	0.0403052	0.435311	0.420367
	-0.2	-0.311221	0.0646837	0.473516	0.38762
	-0.4	-0.344821	0.0737547	0.487708	0.375405
Ec	0.01	-0.239542	0.047573	0.447817	0.409673
	0.03	-0.239626	0.0475803	0.448373	0.409226
	0.05	-0.23971	0.0475875	0.448929	0.408779
	0.07	-0.232595	0.0469144	0.450419	0.407541
A11	0.1	-0.239542	0.047573	0.447817	0.409673
	0.3	-0.239869	0.0476014	0.449864	0.40805
	-0.1	-0.239216	0.0475447	0.445773	0.411294
	-0.3	-0.231625	0.0468287	0.444793	0.412015
B11	0.1	-0.237115	0.047373	0.428597	0.425952
	0.3	-0.237551	0.0474107	0.431336	0.42377
	-0.1	-0.236683	0.0473355	0.425881	0.428115
	-0.3	-0.228696	0.0465826	0.423999	0.429566
Le	1.0	-0.237115	0.047373	0.428597	0.425952
	2.0	-0.237551	0.0474107	0.431336	0.42377
	3.0	-0.236683	0.0473355	0.425881	0.428115
	4.0	-0.228696	0.0465826	0.423999	0.429566
Pr	0.71	-0.239542	0.047573	0.447817	0.409673
	1.71	-0.226719	0.046498	0.350203	0.491672
	3.71	-0.215748	0.0455451	0.273769	0.554697
	7.00	-0.196287	0.0437184	0.216996	0.60053

6.REFERENCES

[1] Agarwal, R.S and Dhanapal, C : Numerical solution to the flow of a micro polar fluid flow through porous walls of different permeability. pp. 325-336 (1987).

[2] Alam, Md, Delower Hossain, M and Arif Hossain, M : Viscous dissipation and joule heating effects on steady MHD combined heat and mass transfer flow through a porous medium in a rotating system. Journal of Naval Architecture and Marine Engineering, V.2, pp.105-120 (2011).

[3] Bachok, N., Ishak, A., Pop, I., Boundary-layer flow of nanofluids over a moving surface in a flowing fluid, International journal of thermal sciences, vol.49, pp.1663-1668, 2010.

[4] Balasubramanyam M : Effect of radiation on convective Heat and Mass transfer flow in a horizontal rotating channel communicated to Research India Publications, India (2010).

[5] Buongiorno, J., Convective transport in nanofluids, J. Heat Transfer 128 (2006) 240 – 250.

[6] Chamkha, A. J., Aly, A. M., and Al – Mudhaf, H., Int. J. Microscale Nanoscale Thermal Fluid Transp. Phenom. 2, 51 (2011).

[7] Choi, S.U.S., Enhancing thermal conductivity of fluids with nano particles, Developments and Applications of Non-Newtonian Flows, FED-vol. 231/MD-vol. 66, 1995, pp. 99-105.

[8] Choi, S.U.S., Zhang, Z.G., Yu, W., Lockwood, F.E., and Grulke, E.A: Anomalously thermal conductivity enhancement in nanotube suspensions, Appl. Phys. Lett. 79, pp.2252-2254(2001).

[9] Circar and Mukharjee : Effects of mass transfer and rotation on flow past a porous plate in a porous medium with variable suction in slip flow. Acta Cienica Indica, V.34M, No.2, pp.737-751 (2008).

[10] Crane, LJ (1970), Flow past a stretching sheet, J. Appl. Math. Phys. (ZAMP) 21: 645 – 647.

[11] Eastman, J. A., Choi, S. U. S., Li, S., Thompson, L. J., and Lee, S., Enhanced thermal conductivity through the development of nanofluids, in: Nanophase and Nanocomposite Materials II, eds. S. Komarneni, J. C. Parker and H. J. Wollenberger, pp. 3 – 11 (1997), Materials Research Society, Pittsburgh.

[12] Eastman, J. A., Choi, S. U. S., Li, S., Yu, W., Thompson, L. J., Anomalously increased effective thermal conductivity of ethylene glycol – based nanofluids containing copper nano particles, Appl. Phys. Lett., 78(6) : (2001) 718 – 720.

[13] El.Mistikawy, T.M.A, Attia, H.A : The rotating disk flow in the presence of Strong magnetic field. Proc. 3rd Int. Congr. of fluid mechanics. Cairo, Egypt. V.3, 2-4 January, pp 1211-1222 (1990).

[14] Gorla, R. S. R. O., and Chamkha, A., Natural convective boundary layer flow over a horizontal plate embedded in a porous medium saturated with a nano fluid, Journal of Modern Physics, vol. 2, pp. 62 – 71, 2011.

[15] Grubka, L. J., and Bobba, K. M., Heat Transfer characteristics of a continuous, stretching surface with variable temperature, J. Heat Transf. 107(1), 248-250 (1985)

[16] Hamad, M. A. A., Ferdows, M., Similarity solution of boundary layer stagnation – point flow towards a heated porous stretching sheet saturated with a nanofluid with heat absorption/generation and suction/blowing: a lie group analysis. Common Nonlinear Sci Numer Simulat 2011, 17(1) : 132 – 140.

[17] Hamad, M.A., Pop, I., Ismail, A.I., Magnetic field effects on convection flow of a nanofluid past a vertical semi-infinite flat plate, Non-Linear Analysis: Real World Applications, vol.12, pp.1338-1346, 2011.

[18] Hazem Ali Attia : Unsteady MHD flow near a rotating porous disk with uniform suction or injection. Fluid dynamics Research, V.23, pp.283-290.

[19] Kamalakar, P.V.S, Prasada Rao, D.R.V : Finite element analysis of chemical reaction effect on non-darcy convective heat & mass transfer flow through a porous medium in vertical channel with heat sources. Int. j. Appl. Math & Mech., V.13, pp.13-28(2012).

[20] Keblinski, P., Phillpot, S. R., Choi, S. U. S., and Eastman, J. A., Mechanisms of heat flow in suspensions of nano – sized particles (nanofluids), Int. J. Heat and Mass Trans, 45(4), 855 - 863 (2002).

[21] Khan, M. S., Karim, I., Ali, L. E., Islam, A., Unsteady MHD free convection boundary- layer flow of a nanofluid along a stretching sheet with thermal radiation and viscous dissipation effects, Int. Nano Lett. 2, 24 (2012)

[22] Khan, WA, Pop, I, Boundary-layer flow of a nanofluid past a stretching sheet. Int. J Heat Mass Transf 53 (2010) 24772483

[23] Kleinstreue, C., J. Li and J. Koo, Microfluidics of nano-drug delivery, Int. J. Heat and Mass Transf. 51(23), 5590-5597 (2008).

[24] Krishna, D.V, Prasada Rao, D.R.V and Ramachandra Murthy, A.S: Hydromagnetic convection flow through a porous medium in a rotating channel, J. Eng. Phys. and Thermo Physics,V.75, No.2, pp.281-291(2002).

[25] Kuznetsov, A. V., Nield, D. A., Natural convective boundary-layer flow of a nano fluid past a vertical plate, Int. J. Therm. Sci. 49 (2010) 243 – 247.

[26] Madhavi.S and Prasada Rao, D.R.V: Effect of chemical reaction and thermo- diffusion on convective heat and mass transfer flow of a rotating fluid through a porous medium in a vertical channel with stretching walls., Int.J.Math. Archives,. 8(5),pp.65-79(2017)

[27] Madhusudhan Reddy. Y, Prasada Rao, D.R.V : Effect of thermo diffusion and chemical reaction on non-darcy convective heat & mass transfer flow in a vertical channel with radiation. IJMA, V.4, pp.1-13 (2012).

[28] Makinde, O. D., Aziz, A., Boundary layer flow of a nanofluid past a stretching sheet with convective boundary condition, Int. J. Therm. Sci. 50 (2011) 1326 – 1332.

[29] Minsta, H. A., Roy, G., Nguyen, C. T., Doucet, D., New temperature dependent thermal conductivity data for water – based nanofluids, Int. J. Thermal Sci. 48 : (2009) 363 – 371.

[30] Mohamed Abd El-Aziz, Effects of Hall current on the flow and heat transfer of a nanofluid over a stretching sheet with partial slip, International Journal of Modern Physics C, Vol. 24, No. 7 (2013) 1350044.

[31] Mohan, M : Combined effects of free and forced convection on magneto hydrodynamic flow in a rotating channel. Proc. Indian Acad. Sc., V.85, pp.383-401 (1977)

[32] Mohan, M, Srivatsava, K.K : Combined convection flows through a porous channel rotating with angular velocity. Proc. Indian Acad. Sci., V.87, p.14 (1978).

[33] Nadeem, S., Lee, C., Boundary layer flow of a nanofluid over an exponentially stretching surface. Nanoscale Res Lett 2012, 7:94.

[34] Prasada Rao, D.R.V, Krishna, D.V and Debnath, L : Combined effect of free and forced convection on MHD flow in a rotating porous channel. Int. J. Math and Math. Sci., V.5, pp.165-182 (1982).

[35] Rana, P., Bhargava, R., Flow and heat transfer of a nanofluid over a nonlinearly stretching sheet: A numerical study, Communications in Nonlinear Science and Numerical Simulation, 2011.

[36] Sarojamma, G and Krishna, D.V : Transient Hydromagnetic convection flow in a rotating channel with porous boundaries. Acta Mechanica, V. 39, p.277 (1981).

[37] Singh, K.D and Mathew : An oscillatory free convective MHD flow in a rotating vertical porous channel with heat sources. Ganita, V.60, No.1, pp.91-110 (2009).

[38] SreenivasaRao:MHD mixed convective heat and mass transfer in a vertical channel with stretching walls., Int.Res and Dev.in Technology.,V.7(4),pp.21-32(2017

[39] Sulochana,C and Ramnakrishna,G.N:Effect of heat sources on non-Darcy convective heat and mass transfer flow of Cuo-water and Al_2O_3-water nanofluids in vertical channel., Int.Jour.Energing trends in engineering and development,V.3(7),pp.52-69,(2017),ISSN.2249

[40] Zanchini, E : Effect of viscous dissipation on mixed convection in a vertical channel with boundary conditions of the third kind. Int. J. of Heat and Mass Transfer, V.41, pp.3949-3959 (1998).